Late Cretaceous to Recent kinematics of SE Anatolia (Turkey)

N. Kaymakci, M. Inceöz, P. Ertepinar and A. Koç

Geological Society, London, Special Publications 2010; v. 340; p. 409-435
doi:10.1144/SP340.18

Late Cretaceous to Recent kinematics of SE Anatolia (Turkey)

N. KAYMAKCI[1]*, M. INCEÖZ[2], P. ERTEPINAR[3] & A. KOÇ[1]

[1]*Middle East Technical University, Department of Geological Engineering, 06531-Ankara, Turkey*

[2]*Fırat Üniversitesi Mühendislik Fakültesi Jeoloji Mühendisliği Bölümü, 23119 Elazığ, Turkey*

[3]*Forthoofddijk Paleomagnetic Lab. Department of Earth Sciences, Utrecht University, Budapestlaan 17, 3584 CD Utrecht, the Netherlands*

**Corresponding author (e-mail: kaymakci@metu.edu.tr)*

Abstract: Five different deformation phases have been recognized in the SE Anatolian orogen and the Arabian Platform based on palaeostress inversion studies using fault-slip data sets. The timing and duration of these phases are determined using various criteria including the age of the affected strata, syndepositional structures, cross-cutting structures and overprinting slickensides. The oldest deformation phase is characterized generally by NE–SW-directed extension. The extension is thought to have resulted from slab-roll back processes during the Maastrichtian to Middle Eocene interval (*c.* 60 Ma to 40–35 Ma). The second deformation phase is characterized by east–west to NW–SE-directed compression and thought to result from cessation of roll-back processes possibly due to subduction of younger oceanic crust or increase in the convergence rate between Africa and Eurasia during the post-Middle Eocene to Late Oligocene interval (*c.* 40–35 Ma to 25 Ma). The third deformation phase is characterized by east–west to NW–SE-directed extension possibly due to slab detachment that initiated in Iran and migrated westwards during the latest Oligocene to Middle Miocene period (25–11 Ma). The fourth deformation phase is characterized by approximately north–south-directed compression due to collision and further northwards indentation of Arabian Plate by the end of Middle Miocene (11–3.5 Ma). The fifth and present deformation phase is characterized by NE–SW compression which might result from tectonic re-organization in the region since the Middle Pliocene (*c.* 3.5 Ma to recent).

The Late Cretaceous to recent tectonic development of SE Turkey is related to the closure of the Neotethys Ocean along two trenches namely the southern and northern branches (Şengör & Yılmaz 1981) while the evolution of these subduction systems partly overlapped in space and time. The Izmir-Ankara-Erzincan Suture Zone (Fig. 1) marks the former position of the northern branch of the Neotethys which separated the Pontides (Eurasian affinity) in the north and the Taurides (Gondwana affinity) in the south. In eastern Turkey, the Taurides are represented by the Keban-Malatya-Bitlis Block (KMBB). The Bitlis–Zagros Suture Zone marks the former position of the Southern Neotethys. During the Mesozoic to pre-Late Miocene, it separated the Taurides from the African–Arabian Plate.

There is still an ongoing debate on the exact location and timing of closure of these two oceanic domains. Nevertheless, it is generally accepted that the closure of the northern branch took place, along the İzmir-Ankara-Erzincan Suture Zone, at the end of the Late Cretaceous (Tüysüz 1999; Kaymakcı *et al.* 2003, 2009) to Early Cenozoic (Şengör & Yılmaz 1981; Görür *et al.* 1984; Robertson *et al.* 2005) and gave way to a widespread southwards thrusting, ophiolitic nappe emplacement and wholesale metamorphism of the KMBB and northern margin of the Taurides. These metamorphic massifs which belong to the northern margin of the Taurides are also known as Anatolides (Ketin 1966). The closure of the southern branch took place along the Bitlis–Zagros Suture Zone during the Middle Miocene (Şengör *et al.* 1985; Yiğitbaş & Yılmaz 1996*a*, *b*; Huesing *et al.* 2009; Kuşcu *et al.* 2010). However, some argued that its closure took place in the Late Cretaceous and the Neogene deformation is related to post-collisional convergence (e.g. Yazgan & Sussex 1991; Bayarslan & Bingöl 2000).

Two contrasting styles of thrusting and nappe emplacement define the current structural architecture of eastern and south-eastern Anatolia in addition to a number of generally NE–SW to NNE–SSW striking strike–slip faults (Fig. 2). These are generally south-verging thrust faults along which much of the ophiolitic masses and slivers belonging to the northern Neotethys Ocean were emplaced onto the KMBB during the Campanian–Maastrichtian (Perinçek & Özkaya 1981). Other important structures are the north-verging thrust faults related to the successive

From: Sosson, M., Kaymakci, N., Stephenson, R. A., Bergerat, F. & Starostenko, V. (eds) *Sedimentary Basin Tectonics from the Black Sea and Caucasus to the Arabian Platform.* Geological Society, London, Special Publications, **340**, 409–435. DOI: 10.1144/SP340.18 0305-8719/10/$15.00

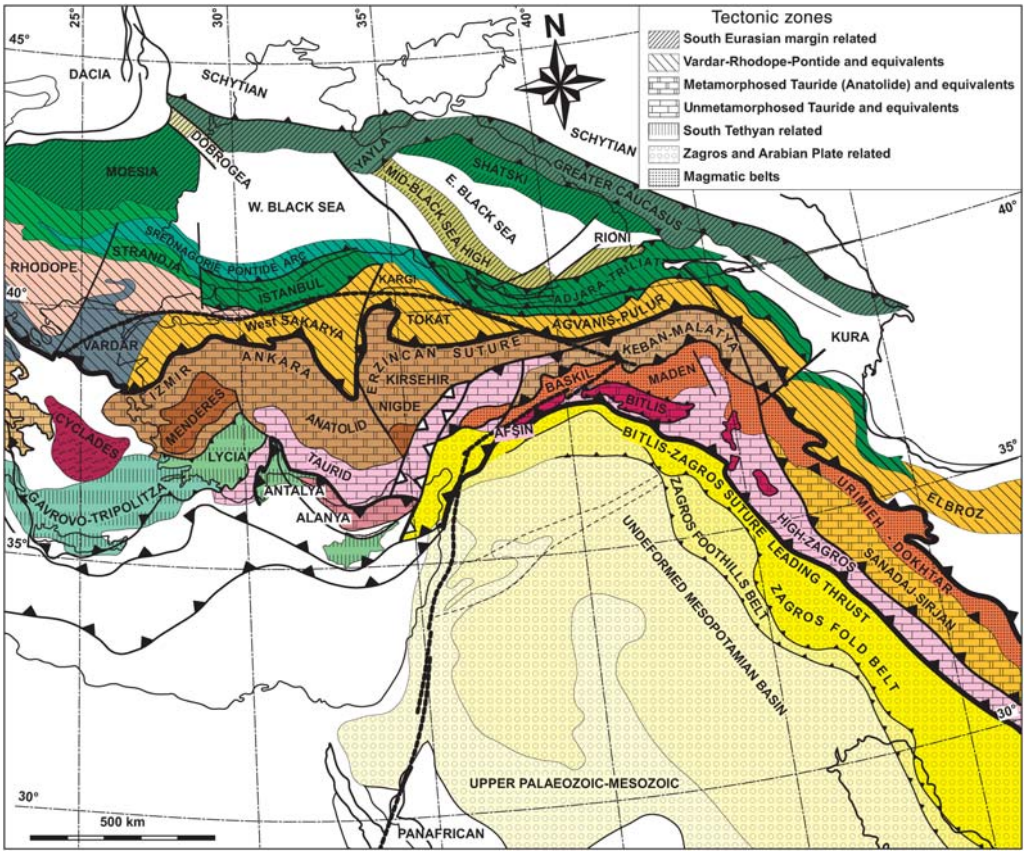

Fig. 1. Regional tectonic units around Turkey (modified from Okay *et al.* 1994; Stampfli & Borel 2002). Note that Menderes, Kırşehir, Alanya, Keban-Malatya and Bitlis units are also known as Anatolides (Ketin 1966) which are the metamorphosed equivalents of Taurides (Şengör & Yılmaz 1981). Note also that Sakarya-Tokat-Kargı, Agvanis-Pulur massifs are part of Rhodope-Pontide Fragments. The Baskil, Maden and Urimeh-Doktar belts belongs to Late Cretaceous to Eocene arc and back arc settings of Bitlis–Zagros Suture zone.

collision of an island arc chain (Afşin-Baskil arc) during the Late Cretaceous, located between the KMBB and the Arabian Block (Figs 1 & 2c), within the southern branch of the Neotethys.

Terminal collision of the Arabian Plate produced approximately north–NE-striking transcurrent faults which translated Late Miocene to Middle Pliocene thrust faults more than 100 km along their strike. Due to bivergent thrusting, which is due south in the south and due north in the north, gave way to pop-up-like uplift of the KMBB during the Late Miocene to Middle Pliocene (Fig. 2c). The recent studies indicated that the evolution of the region is rather complex. Various ophiolitic and magmatic units in the region are originated from different tectono-magmatic settings including processes possibly related to slab roll-back, slab detachment, supra-subduction zone ophiolite generation during the northwards subduction of southern branch of the Neotethys (e.g. Yiğitbaş & Yılmaz 1996*a*, *b*; Robertson 2002; Parlak 2004; Parlak *et al.* 2004, 2006; Robertson *et al.* 2005; Faccena *et al.* 2005; Kuşcu *et al.* 2010).

The active tectonic scheme of the region is related to (1) the detachment of the subducting oceanic lithosphere at the northern end of the Arabian plate; (2) development of a Subduction Transform Extension Propagator (STEP) fault (cf. Govers & Wortel 2005) along the northwestern margin of the Arabian Plate (Facenna *et al.* 2005); and (3) collision and further northwards convergence of the Arabian Plate by the end of the Middle Miocene (*c*. 11 Ma) (Şengör *et al.* 1985; Dewey *et al.* 1986; Huesing *et al.* 2009). These processes gave way to inversion of most of the pre-existing structures and development of a number of NNE–SSW to ENE–WSW striking strike–slip fault systems (Perinçek *et al.* 1987; Westaway & Arger

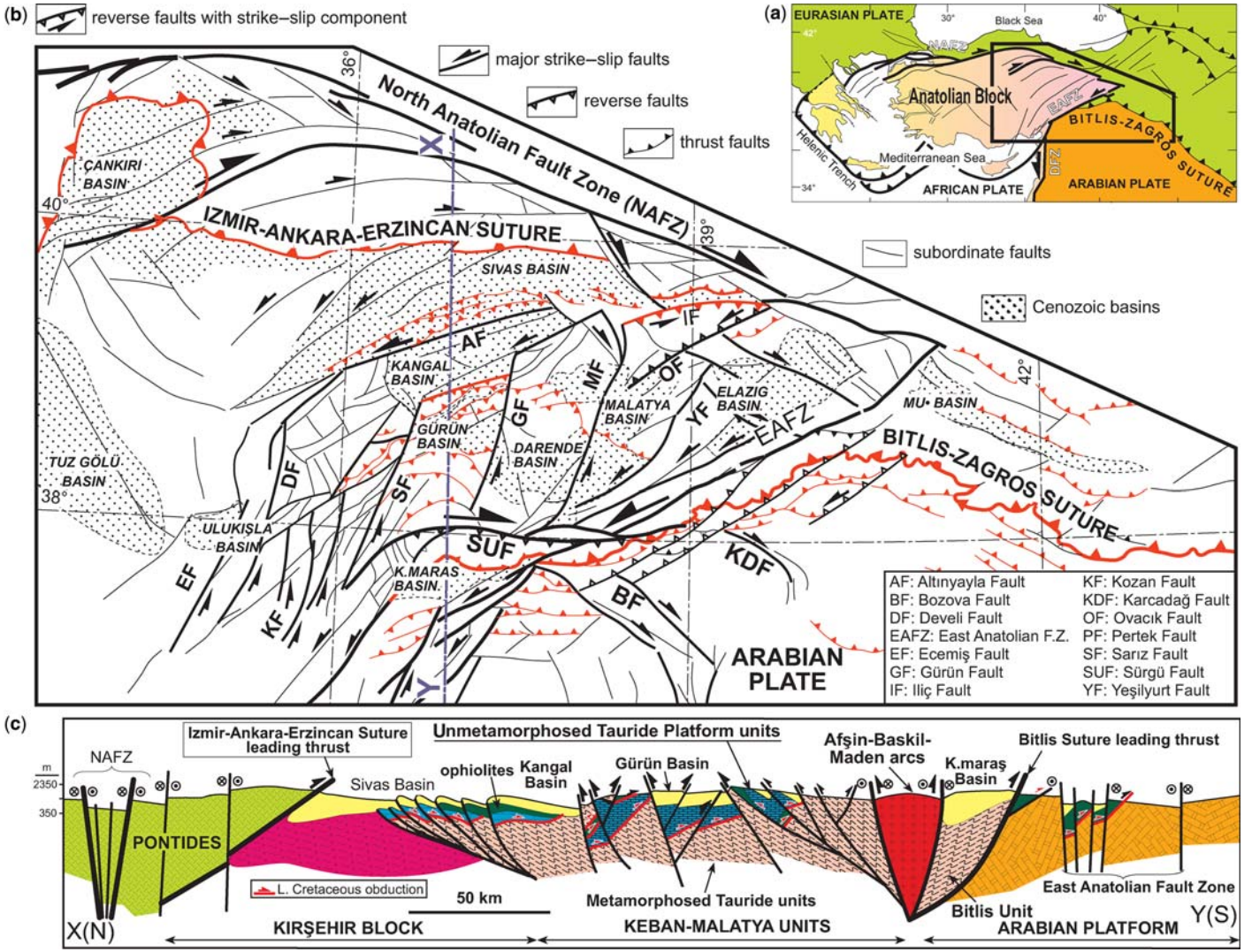

Fig. 2. (**a**) Outline active tectonics of Turkey. (**b**) Major palaeotectonic (red) and neotectonic (black) structures and Cenozoic basins in central and southeastern Turkey. (**c**) Simplified regional cross-section along the line XY.

2001; Kaymakcı *et al.* 2006) in response to STEP faulting, north–south shortening, crustal thickening (Dewey *et al.* 1986) and westwards escape of the Anatolian Block (Şengör *et al.* 1985).

The aim of this study is to present Late Cretaceous to recent kinematic evolution of SE Anatolian Orogen and the northwestern part of the Arabian Platform in order to constrain the timing, mechanism and extend of processes related to subduction of the southern Neotethys Ocean and collision and further northwards convergence of Arabian Plate. The SE Anatolian Orogen, here, refers to the area north of the Bitlis–Zagros Suture and south of Izmir-Ankara-Erzincan Suture Zone in Turkey (Yılmaz 1993).

Tectono-stratigraphy

The tectonic units that played a role in the development of the region include the Arabian Platform, Bitlis Massif, Keban-Malatya Platform, non-metamorphosed Tauride Platform units, and various ophiolitic and magmatic complexes comprising Afşin-Baskil arc and Maden complex (Figs 1 & 2). These units are tectonically imbricated along north dipping thrust faults and are unconformably overlain by marine to continental carbonates and clastics deposited during the Cenozoic (Figs 2–4).

Stratigraphy of the Arabian Platform

The Arabian Platform comprises sedimentary successions ranging from Precambrian to Recent (Fig. 3). It is generally accepted that it was located at the northern margin of the Gondwana from the Precambrian to the Late Palaeozoic. The Arabian Platform constituted the southern passive margin of the Southern Neotethys Ocean after rifting and northwards drifting of the Taurides from its northern margin during the Mesozoic to Palaeogene (Şengör & Yılmaz 1981).

The oldest compressional structures on the platform are related to the emplacement of ophiolitic units during the Campanian to Maastrichtian (Perinçek & Özkaya 1981). These structures and thrust contacts are sealed by the Late Maastrichtian to Paleocene and younger units. The important youngest structures that shape the present structural grain of the platform are related to the late Miocene collision and preceding foreland basin development. In this study, we concentrated mainly on the post-Maastrichtian kinematic events within the platform.

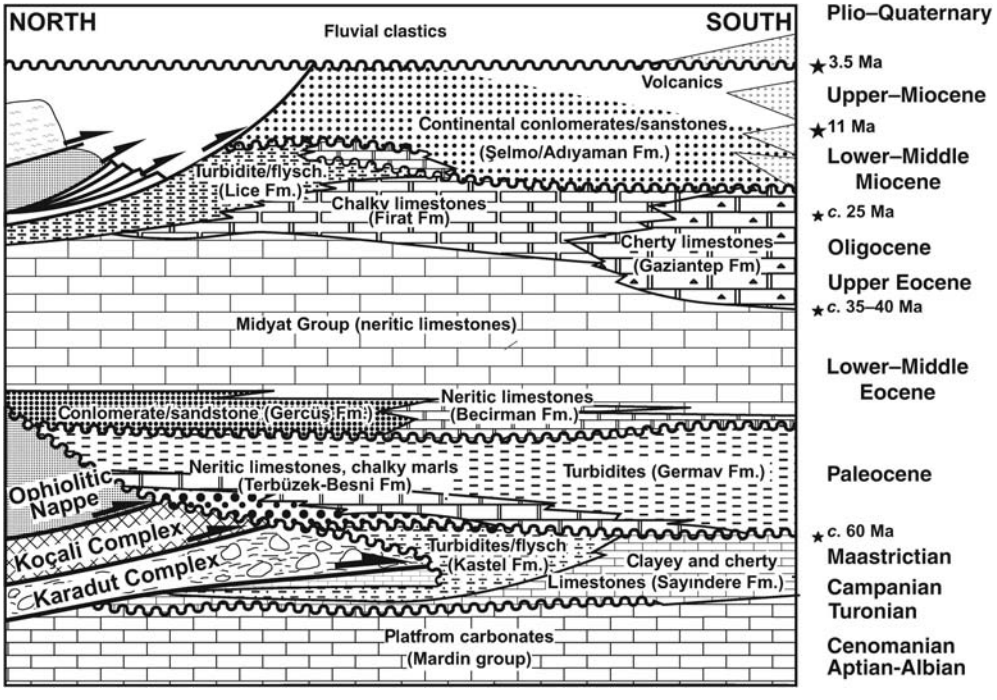

Fig. 3. Generalized Cretaceous to Recent tectonostratigraphical column of Arabian Platform in Turkey (modified from Perinçek & Özkaya 1981; Yılmaz 1993). Absolute ages correspond to the beginning of deformation phases mentioned in the text.

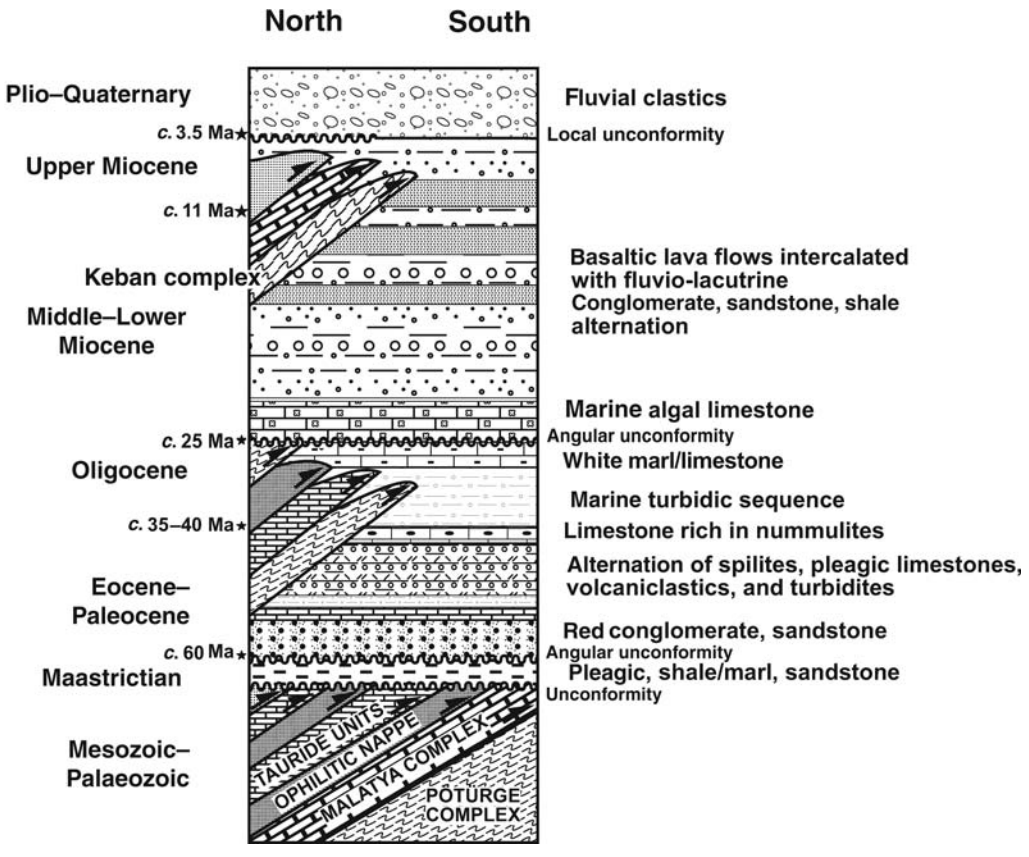

Fig. 4. Generalized Maastrichtian to Recent tectono-stratigraphical column of SE Anatolian orogen (modified from Yiğitbaş & Yılmaz 1996*a*).

The sampled interval on the Arabian Platform ranges in age from Maastrichtian to Pliocene and includes a facies association, from bottom to top, few tens of metres thick continental red clastics (Terbüzek Formation), chalky marls (Besni Formation), a turbiditic sequence (Germav Formation) composed of alternation of sandstone, siltstone and shale. These facies are overlain by clastics (Gercüş Formation) and about ten metres thick neritic limestone (Becirman Formation) (Yılmaz 1993). These units are unconformably overlying the older units and seals the thrust contact between the late Cretaceous emplaced ophiolitic melanges.

The thickness of the turbidites (Germav Formation) increases northwards as the grain sizes become coarser and comprises olistostrommal conglomerate lenses. In the southwestern part of the study area, the Paleocene rocks unconformably overlies the ophiolitic units (Karadut & Koçali complexes) which indicates that these units are deposited after the Campanian–Maastrichtian emplacement of the ophiolitic units onto the Arabian Platform. The Paleocene association is unconformably overlain by Eocene to Lower Miocene rock units. The Eocene to Lower Miocene units have very rapid lateral and vertical facies changes in different parts of the Arabian Platform. Therefore, in the literature, various local names are used for these units. For simplicity we followed the nomenclature of Sungurlu (1974) and Perinçek (1979) who collectively named the Eocene clastic sequence as the Gercüş Formation and overlying carbonates as the Midyat Limestone. The Eocene clastic sequence (Gercüş Formation) is composed of various clastics including conglomerates, sandstones and mudstones gradually fining upwards as the depositional environments are changing from continental to marine settings. The overlying carbonates (Midyat Limestone) comprise three distinct levels. The lower level is composed of dolomitic limestones that gradually grade into limestones with cherty intervals and limestones with cherty nodules. These levels are also known as Gaziantep Formation (Wilson & Krummenacher

1957). The cherty levels upwards grade into the medium- to thick-bedded marl, chalky limestone alternations with occasional cherty nodules. This uppermost chalky limestone part of the Midyat Formation is also named as Fırat Formation along the northern edge of the Arabian Plate and is early to Middle Miocene in age (Perinçek 1979). The Fırat Formation also comprises tuff layers in its lower parts and grades northwards laterally into turbidites (Lice Formation) (Tuna 1973; Sungurlu 1974; Perinçek 1979; Perinçek & Özkaya 1981).

The Lower to Middle Miocene Turbidites (Lice Formation, Tuna 1973) comprises northwards and upwards coarsening turbidite facies. It is developed mainly in front of the south-directed thrust faults at the northern edge of the Arabian Platform along the leading edge of the Bitlis–Zagros Suture. It is generally accepted that these turbidites (Lice Formation) mark the terminal stage of subduction of the Southern Branch of the Neotethys and beginning of collision of the Arabian Plate (Şengör & Yılmaz 1981). They are conformably overlain by continental red clastics which are known also as Şelmo (Perinçek 1979) and Adıyaman (Tuna 1973) formations (Fig. 3) in the northeastern and northwestern parts of the Arabian Platform respectively.

A very widespread isolated alkaline basaltic lava flows are emplaced onto the Arabian Platform. These basaltic lava flows can be subdivided into three distinct groups. The oldest lava flows are observed around the western margin of the Arabian Platform and have lateral gradations with the Fırat Formation. The K–Ar ages of these volcanic rocks range between 21.24 ± 2.04 to 9.22 ± 0.2 Ma (Yoldemir 1987; Tatar *et al.* 2004). The second group is exposed in the central part of the Arabian Platform and are unconformably overlying the Fırat Formation and their K–Ar ages range between 12.1 ± 0.4 to 7.02 ± 0.07 Ma (Yoldermir 1987; Ulu *et al.* 1991). The third and youngest group belongs to the Karacadağ Volcanic Complex and their K–Ar ages range between 0.94 ± 0.33 to 0.83 ± 0.88 (Pearce *et al.* 1990).

Stratigraphy of the SE Anatolian orogen

The sampled intervals within the SE Anatolian orogen range in age from Maastrichtian to Early Quaternary. The Eocene volcanic and volcaniclastic rocks of the Maden Complex were not studied for palaeostress analysis. The reason for this is because, in the volcanic fields local stress variations are unpredictable and they reflect local stress fields rather than regional stress configurations due to rapid deposition and extensive local vertical movements during volcanic eruptions. However, contemporary sedimentary sequences were studied in detail (Fig. 4).

The Maastrichtian to Paleocene sequences have lateral and vertical facies changes ranging from turbidites (Gürer & Aldanmaz 2002) to pelagic limestones to shallow continental red clastics (Aziz *et al.* 1982; Perincek & Kozlu 1984). Around the Darende Basin (Fig. 2b), at the bottom, these sequences rest on ophiolitic units with an unconformity and are composed of turbiditic facies comprising conglomerate, sandstone, siltstone and shale alternations which grades upwards into shallow marine limestones. In the southern margin of the Malatya Basin, these units are Maastrichtian in age and are composed of alternation of pelagic limestones and marls intercalated with thin sandstones.

The Upper Maastrichtian sequences are unconformably overlain by the Upper Paleocene continental red clastics comprising red to purple conglomerates and sandstone sequences. The lower part of the Upper Paleocene sequence is always associated with normal growth faults (Fig. 5). In the southern margin of the Malatya Basin, this sequence is about 100 m thick and rapidly grades into boulder conglomerates and sandstones which subsequently grades upwards into turbiditic facies alternating with nummulites bearing limestone horizons. This sequence is overlain by Oligocene shallow marine limestones only to the western margin of the Malatya Basin. However, within and in the eastern margin of the Malatya Basin, Oligocene sequences are missing. In these areas, Lower Miocene sequences directly rest either on the metamorphic basement or onto the Eocene sequences.

The Lower Miocene sequences start at the bottom with few metres thick shallow marine shales and marls which continues upwards with few tens of metres thick condensed sequence of shallow marine algal limestones. The condensed sequences are conformably overlain by Middle Miocene lacustrine facies in the Malatya and Gürün basins (Figs 2 & 4). The lacustrine sequences grade upwards into fluvio-lacustrine clastics intercalated with coal seams and into a volcano-clastic sequence in the northern part of the Malatya Basin. Based on rodent fauna (Kaymakcı *et al.* 2006) and 15.2–15.9 Ma (Arger *et al.* 2000) K–Ar ages from the inter-layered lava flows these sequences are of Middle to Late Miocene in age. In the Kangal Basin (Fig. 2), deposition of these sequences continued until the Early Pliocene. All these sequences are unconformably overlain by the Upper Pliocene to Pleistocene fluvial clastics.

Palaeostress inversion

Palaeostress analysis aims at the reconstruction of palaeostress configurations using fault-slip data

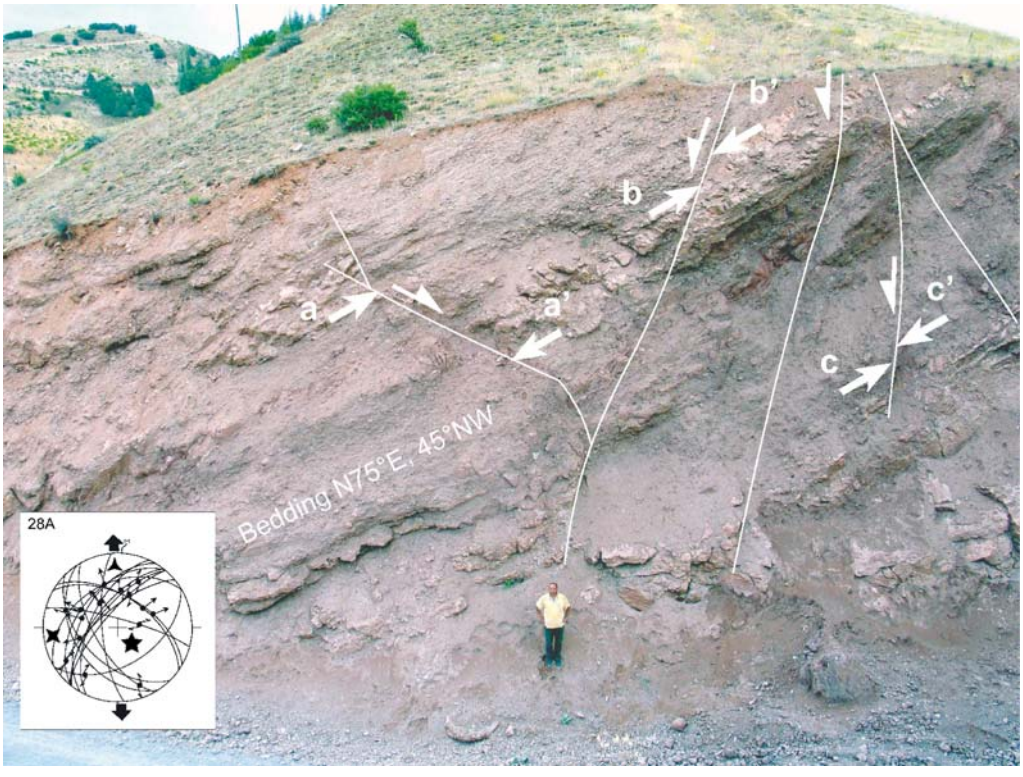

Fig. 5. Growth faults developed within the Paleocene clastics (location: Site 28 in Fig. 6, view to NE) and their palaeostress configuration. Note that north–south extension of the growth faults.

sets (Angelier 1994). The back bone of the method is based on the assumption that the slip occurs parallel to the maximum resolved shear stress along an optimally orientated plane of weakness (Wallace 1953; Bott 1959). Basically, there are two types of palaeostress inversion techniques. The graphical approaches generally based on Anderson's (1951) fault theory which states that the maximum principal stress is the acute-bisetrix of conjugate fault sets while minor stress is the obtuse-bisetrix and intermediate stress is parallel to the intersection of conjugate fault planes. This approach is based on the fact that the earth's surface is one of the principal planes so that one of the stresses is always vertical. This implies that oblique-slip faults are always re-activated planes of weaknesses. In this approach, the most reliable results can only be obtained in the case of conjugate faults which are, most of the time, very difficult to determine during field studies. On the other hand, the numerical methods are based mainly on the reconstruction of the stress ellipsoid by using the Wallace (1953)–Bott (1959) assumption. In this approach slip occurs along the maximum resolved shear stress along a pre-existing plane of weakness. Therefore, maximum resolved shear stress direction corresponds to the slip direction which is manifested on the plane as slickenlines (Angelier 1994). During the construction of the palaeostress configurations, the maximum shear stress direction is determined by calculating the axes of the stress ellipsoid by using the shape factor ($\phi = \sigma_2 - \sigma_3/\sigma_1 - \sigma_3$). In which σ_1, σ_2 and σ_3 correspond to maximum, intermediate and minor principal stress magnitudes, respectively.

In this study, we have applied only the numerical method developed by Angelier (1988). The method is based on the calculation of a reduced stress tensor which means that the relative magnitudes and orientations of the principal stresses are determined by using the shape factor and orientation of at least four fault slip data belonging to the same deformation phase (see Angelier 1994 for a full account of the method).

In addition to direction and magnitudes, one of the other key issues in palaeostress analysis is the dating of the constructed stress configurations. This is accomplished by using various criteria that

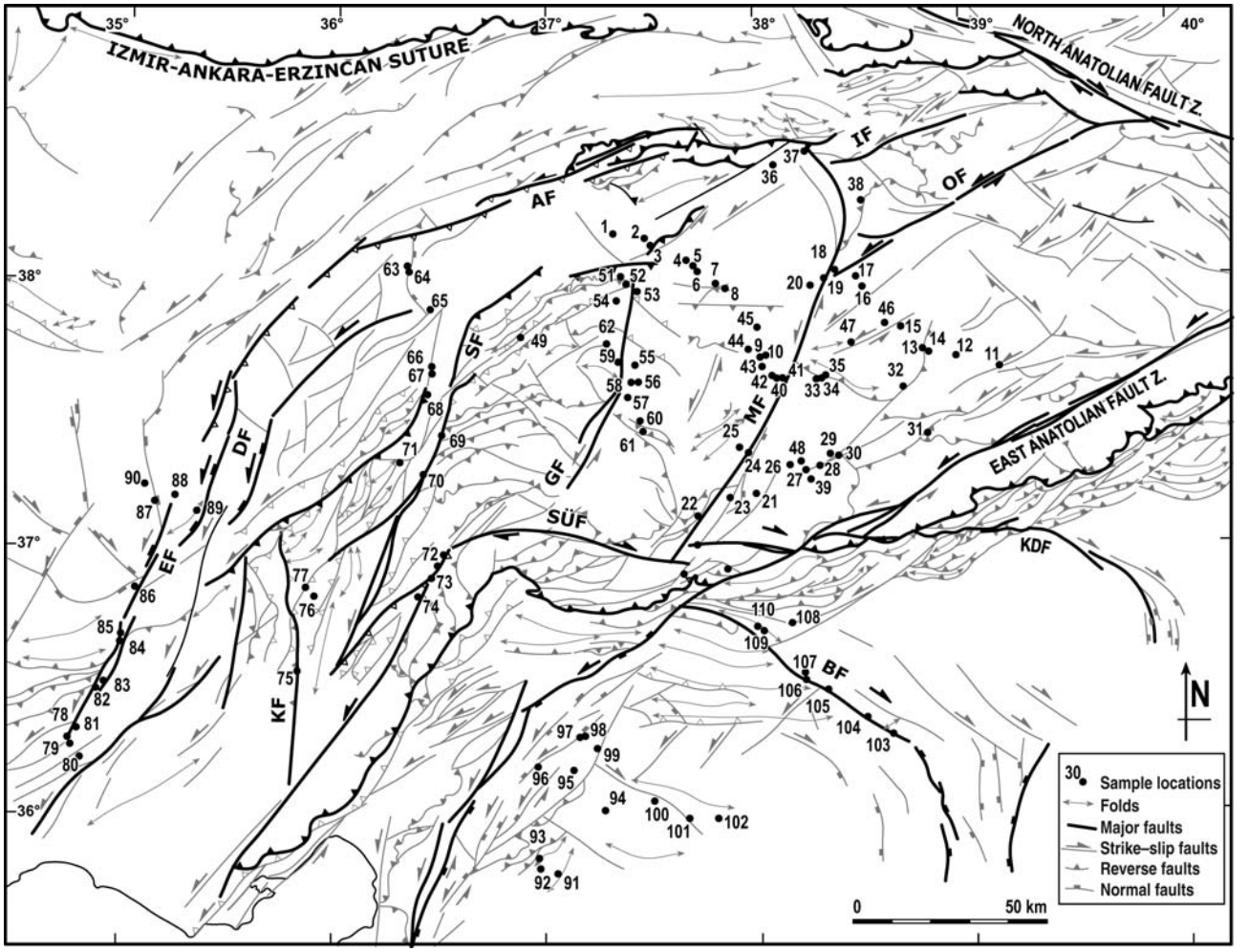

Fig. 6. Major faults and sample locations of the study area. Fault names are as in Figure 2.

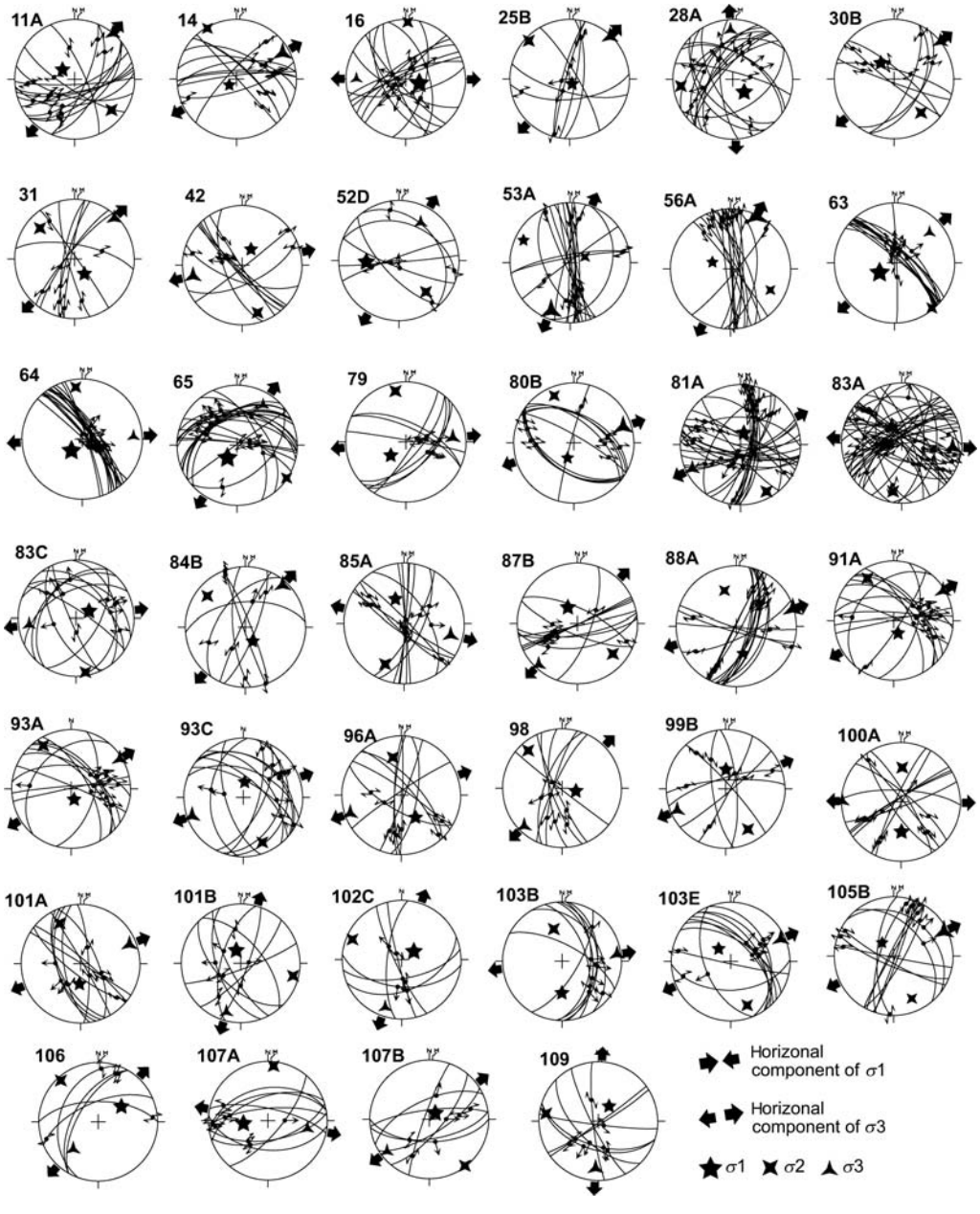

Fig. 7. Palaeostress configurations belonging to Paleocene to Middle Eocene extension (phase 1). Note that sites 91–107 belong to the Arabian Platform, all others belong to SE Anatolian orogen. Equal area, lower hemisphere projection.

include, in decreasing order of reliability, synsedimentary structures and faults, the age of the youngest faulted strata and age of the oldest sealing strata, age of the youngest sequences displaced by a specific fault or fault sets (if no seal is discernable), any incompatible compressional structure overprinted or displaced by an extensional structure (or vice versa), overprinting kinematic indicators within the same fault plane, and overprinting slickensides (Kaymakcı *et al.* 2000).

Deformation phases

Arabian Platform

The oldest syn-sedimentary structures are observed with in the Germav Formation in the southwestern part of the study area (site 3 in Fig. 6). In this area, a number of synsedimentary normal faults with graben-horst morphology are observed. Most of the horsts and grabens were tilted possibly due to successive tectonic events. During the palaeostress analyses these structures were tilt corrected. During correction, mean bedding plane attitudes were used as the palaeo-horizontal surface. In the case of listric normal faults, along which differential rotation about horizontal axes is expected, bedding planes of the footwall blocks were used.

From the Upper Maastrichtian to Eocene sites, 17 palaeostress configurations are constructed (Fig. 7, Table 1). Based on this data it is concluded that the region has experienced NE–SW extension during the Paleocene to Eocene. This phase of extension is accepted to be the first phase of deformation after the Campanian–Maastrichtian emplacement of the ophiolitic units on to the Arabian Platform (Perinçek & Özkaya 1981). Since Midyat Formation was deposited during the Eocene to Early Miocene interval, the upper boundary of this phase could not be constrained precisely and it is accepted roughly as Eocene based on the correlation of stress configurations with the other regions (see below).

In most of the sites overprinting slickensides indicating compressional deformation were also observed. These slickensides were constrained mainly to the Upper Eocene–Oligocene (Gaziantep Formation) and older units. In addition to this, a new set of extensional structures characterized generally by growth faults are also observed within the chalky limestone and volcanogenic parts of the Fırat Formation (Fig. 8). The orientation of palaeostress configurations constructed from the growth faults within the Fırat Formation yielded different extensional stress configurations compared to the ones observed in the Upper Cretaceous to Paleocene units. These stress configurations, as being postdating compressional structures observed in pre-Oligocene units are developed within the Lower part of the Fırat Formation (Lower Miocene). This indicates a new phase of extension. In addition, in the Malayat Basin it is well documented by Kaymakcı *et al.* (2006) that this extensional

Table 1. *Geographical coordinates and palaeostress orientations for the phase 1*

Site code	X*	Y*	σ1 (D/P)†	σ2 (D/P)	σ3 (D/P)	Φ‡	N§
11A	39.161	38.674	309/69	130/21	40/00	0.51	14
14	38.804	38.741	231/77	330/02	61/13	0.84	11
16	38.509	38.978	107/71	02/05	270/19	0.16	14
25B	37.919	38.383	153/83	313/07	044/02	0.65	7
28A	37.231	37.254	138/67	263/14	357/19	0.34	10
30B	38.357	38.348	320/61	141/29	051/00	0.56	8
31	38.357	38.348	146/66	312/24	44/04	0.54	8
42	38.097	39.425	029/65	162/18	258/17	0.68	9
52D	37.373	39.015	268/45	139/32	30/28	0.33	6
53	37.442	38.968	296/15	68/68	202/15	0.97	16
56	37.456	38.634	290/64	118/26	26/3	0.98	14
63	36.334	39.046	237/66	140/3	49/24	0.15	12
64	36.330	39.055	223/69	353/14	87/16	0.20	17
65	36.442	38.904	217/69	124/2	33/21	0.16	21
79	34.761	37.260	228/62	348/15	85/23	0.55	8
80B	34.813	37.209	203/68	338/16	72/15	0.86	9
81A	34.792	37.322	341/73	134/15	226/8	0.41	31
83A	34.916	37.497	70/48	185/21	290/35	0.54	35
83D	34.916	37.497	13/80	103/0	193/10	0.83	7
84B	34.990	37.649	153/69	309/20	42/8	0.68	7
87B	35.141	38.172	329/65	130/24	223/7	0.47	10
88A	35.235	38.200	166/52	342/38	73/2	0.86	15
95A	38.008	38.829	221/68	73/19	339/11	0.48	8
100A	38.155	38.317	176/47	003/42	34.13	0.11	9

*X,Y, coordinates in decimal degrees.
†D/P, direction/plunge.
‡Φ, shape factor.
§N, number of faults.

Fig. 8. Growth faults developed within the Upper Oligocene–Lower Miocene Fırat Formation. Note increase in throw from a–a′ to c–c′. (Site 94 in Fig. 6, view to west).

deformation phase started at the end of Oligocene and lasted until the Middle Miocene. Based on this information, it is concluded that the extensional structures belong to deformation phase 3 which took place possibly latest Oligocene to Middle Miocene. Therefore, the compressional structures predating phase 3 and postdating phase 1 are classified into deformation phase 2 and thought to have taken place during the post-Middle Eocene to pre-Latest Oligocene. The palaeostress configurations and stress orientations for phases 2 and 3 are depicted in Figures 9 and 10 and Tables 2 and 3.

Within the Middle to Upper Miocene Adıyaman Formation a very well developed mesoscopic thrust fault occasionally with overprinting slickensides was observed. The older slickensides were related to generally east–west-striking conjugate thrust faults dipping 45° to 20° due north and due south. The hanging wall and footwall blocks of these thrust faults were displaced locally by NE–SW-trending strike–slip faults. The palaeostress configurations for these thrust faults, older overprinted slickensides, and the younger overprinting slickensides were expectedly found to be different

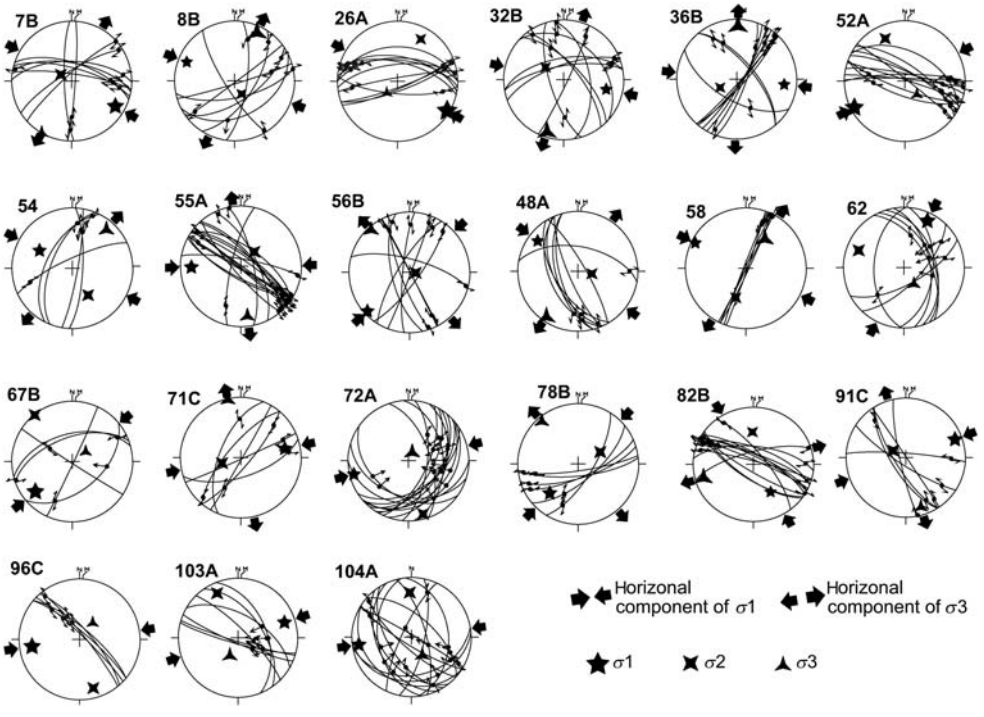

Fig. 9. Palaeostress configurations belonging to Late Eocene–Oligocene compression (phase 2). Note that sites 91–104 belong to the Arabian Platform, all others belong to SE Anatolian Orogen. Equal area, lower hemisphere projection.

(Figs 11 & 12 and Tables 4 & 5). Based on this information, it is interpreted that the reverse faults predate the strike–slip faults and they belong to a new phase of deformation (phase 4) that took place during the deposition of the Şelmo and Adıyaman formations in the Late Miocene to Pliocene. Both the hanging wall and footwall blocks of the thrust faults were displaced by these strike–slip faults, therefore, they can not be tear faults of the thrust faults. Based on this observation it is concluded that the strike–slip faults and younger overprinting slickensides should belong to the younger phase of deformation (phase 5) which has been active since the Middle Pliocene (*c*. 3.5 Ma) as proposed by Kaymakcı *et al.* (2006).

SE Anatolian orogen

In the western and southern margin of the Malatya Basin and southeastern margin of the Ulukışla Basin (Fig. 2) well-developed growth faults were observed where Paleocene to Middle Eocene sequences directly rest on to the older units. For example in sites (27–30 and 39) at the contact between the basement metamorphics and the Maastrichtian to Paleocene red clastics a number of growth faults were observed (Fig. 5). Also in the southern margin of the Malatya Basin around sites 30–31 growth faults are observed at the contact between the Paleocene and Eocene units (Fig. 13). Similar relationships are also observed in various localities throughout the region. Based on these information it is concluded that Maastrichtian to Middle Eocene rocks in the region are deposited during a phase of extensional deformation (phase 1) which might have started during the end of Maastrichtian and continued until the Middle Eocene. The stress configurations for each sites for the deformation phase 1 is depicted in Figure 7 and Table 1.

Within the Oligocene units a number of mesoscopic faults were observed. Some of these faults have overprinting slickensides. However, no diagnostic features that could be used for dating the activity of these faults were not observed during the field studies. On the other hand, a number of normal growth faults were observed within the Lower to Middle Miocene units. For example, in the western margin of the Malatya Basin, at an unconformable boundary between the

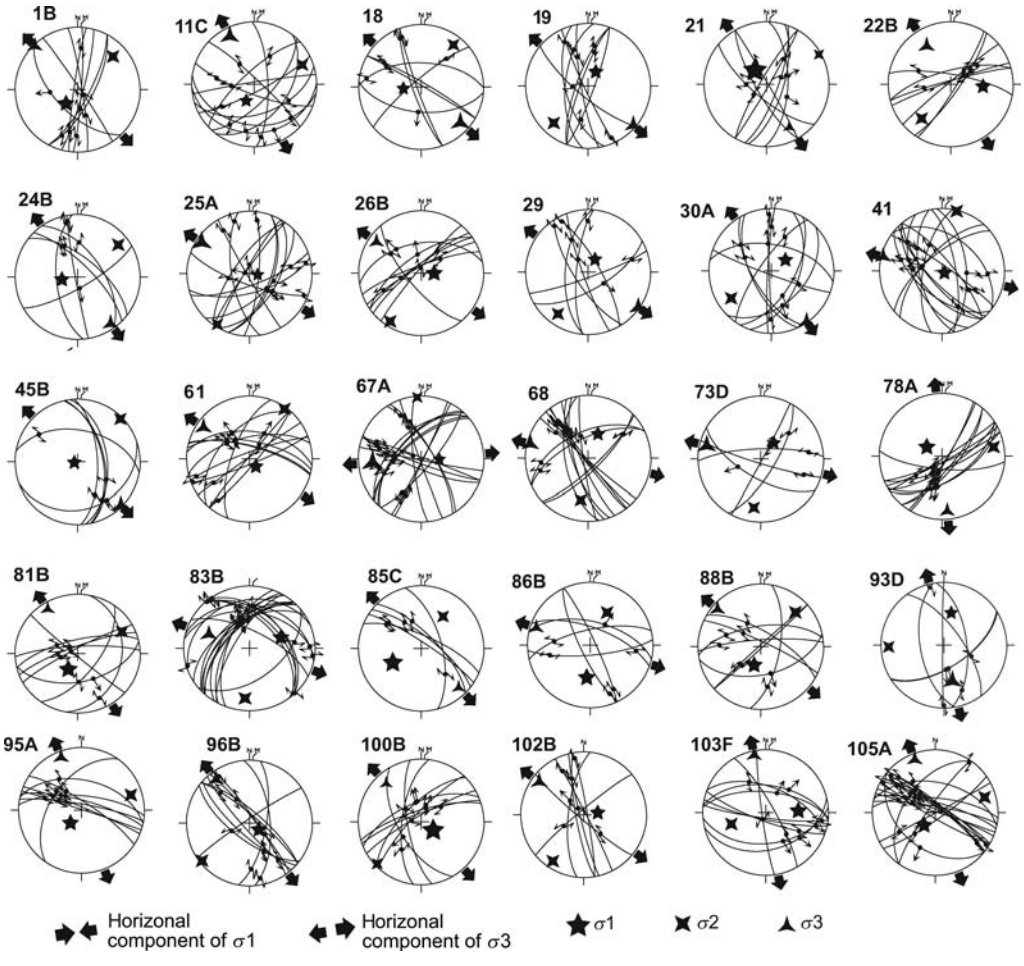

Fig. 10. Palaeostress configurations belonging to latest Oligocene to Middle Miocene extension (phase 3). Note that sites 93–110 belong to the Arabian Platform, all others belong to SE Anatolian orogen. Equal area, lower hemisphere projection.

Eocene limestones and Lower Miocene limestones, numerous normal faults were observed. Some of the normal faults displaced the Eocene units while they do not propagate into the Miocene units. Palaeostress configurations constructed from the faults displacing only the Eocene units and the ones displacing both Eocene and Miocene units expectedly yielded completely different stress configurations. In addition, the stress configurations for the ones sealed by Miocene and those displaced the Miocene rocks are similar to the orientations of the deformation phase 1 and to deformation phase 3 configurations, respectively. At this locality and elsewhere overprinting slickensides indicating reverse faulting are observe within the Eocene and older units. The palaeostress orientations constructed from the younger slickensides and those observed within the Oligocene units found to be similar. In addition to this, around the southern margin of the Gürün Basin (Fig. 2) a number mesoscopic thrust faults were observed between the Mesozoic and Eocene units. These thrust faults are sealed by Middle Miocene lacustrine deposits of the Gürün Basin. Similar relationships are also observed around the sites 50–90 around Gürün, Sarız and Ecemiş faults (Fig. 2). Considering extensional nature of deformation during the Paleocene to Middle Eocene and age of the sealing lithologies as being Miocene, it is concluded that compressional deformation observed within the Eocene and Oligocene units indicates that a phase of compressional deformation took place

Table 2. *Geographical coordinates and palaeostress orientations for the phase 2*

Site code	X*	Y*	$\sigma 1$ (D/P)†	$\sigma 2$ (D/P)	$\sigma 3$ (D/P)	Φ‡	N§
7B	37.813	38.991	120/17	301/73	210/00	0.36	9
8B	37.856	38.972	291/16	152/70	25/12	0.92	8
23	37.865	38.189	164/13	269/50	064/37	0.32	6
26A	37.787	36.996	121/05	029/21	223/68	0.12	11
32B	38.807	38.427	103/28	305/60	198/10	0.88	10
36B	36.957	37.183	096/22	243/65	001/13	0.92	10
48	37.976	38.745	205/10	352/781	114/06	0.79	5
52	37.373	39.015	242/6	335/24	138/65	0.25	12
54	37.334	38.938	298/38	150/47	41/16	0.65	5
55	37.427	38.688	269/19	43/63	173/18	0.58	17
56B	37.456	38.634	227/6	94/82	318/6	0.63	8
58	37.437	38.622	297/7	199/47	33/42	0.82	5
59B	37.359	38.705	271/25	97/65	2/3	0.44	6
62	37.289	38.770	27/14	291/21	148/64	0.43	8
67B	36.455	38.665	231/22	321/1	54/68	0.33	5
71C	36.306	38.322	78/26	254/64	348/2	0.60	6
72	36.465	37.902	256/8	165/9	25/78	0.67	16
78B	34.749	37.287	224/33	62/56	319/8	0.56	6
82A	34.877	37.470	149/43	358/43	254/15	0.86	13
96C	38.328	38.644	261/22	164/18	38/61	0.34	5
104E	38.497	37.368	263/3	355/33	168/57	0.30	18

*X,Y, coordinates in decimal degrees.
†D/P, direction/plunge.
‡Φ, shape factor.
§N, number of faults.

after Eocene (phase 1) and before the Miocene (phase 3) extension phases. Therefore, phase 2 was concluded to have taken place during Late Eocene–Oligocene interval.

Early Miocene to recent palaeostress evolution of Malatya Basin is discussed in Kaymakcı *et al.* (2006). Therefore, in this study we are concentrated on the regions to the west of Malatya Basin. Similar to Malatya Basin within the Late Miocene to recent units a number of large scale and of mesoscopic scale faults with reverse and strike–slip character are observed. One of the most prominent of these structures is observed at the southern margin of Kangal Basin which is delimited by a thrust fault along which the Upper Cretaceous opholitic melange thrust over the Upper Miocene (Messinian) to Lower Pliocene infill of the Kangal Basin (Fig. 14).

In addition to this, along the Sarız Fault a number of strike–slip faults with reverse components are observed within the Upper Miocene to Pliocene units. Similar relationships are also observed within the Ecemiş Fault where strike–slip faults displaced the Upper Miocene units are sealed by Plio-Quaternary deposits.

Likewise, the Plio-Quaternary deposits are locally displaced by mesoscopic faults. The ages of these units are not well constrained. Therefore, the fault-slip data collected from these units are separated and analysed independently. They produced completely different stress configurations compared to the ones observed within the Upper Miocene to Pliocene units. Therefore, we followed the deformation phase schema outlined in the previous section and concluded that the deformation phase 4 corresponds to Late Miocene to Early Pliocene interval and the deformation phase 5 commenced at the Middle Pliocene (*c*. 3.5 Ma) and is still active (see also Kaymakcı *et al.* 2006).

Discussion

As discussed above, in the eastern and southeastern Anatolia five different deformation phases have been recognized (Figs 15–19). The duration of these phases are constrained by using various stratigraphical, structural and kinematic criteria as outlined in Angelier (1994) and Kaymakcı *et al.* (2000). The oldest deformation phase is characterized by generally NE–SW directed extension both in the Arabian Platform and north of it (phase 1). Together with stratigraphical information, this information suggests that the extensional deformation is not a local phenomenon but extends from the Arabian Platform to the eastern Turkey

Table 3. *Geographical coordinates and palaeostress orientations for the phase 3*

Site code	X*	Y*	σ1 (D/P)†	σ2 (D/P)	σ3 (D/P)	Φ‡	N§
1B	37.321	39.184	220/66	47/23	316/02	0.47	8
11C	39.161	38.674	206/66	68/18	333/15	0.76	11
18	38.415	39.028	265/67	37/16	132/16	0.78	7
19	38.333	39.008	028/69	223/20	131/05	0.62	8
21	37.992	38.213	321/66	060/04	152/23	0.01	8
22B	37.849	38.139	094/47	220/29	328/29	0.56	7
24B	37.957	38.357	261/69	052/18	145/09	0.55	6
25A	37.919	38.383	096/79	212/05	303/10	0.87	13
26B	37.787	36.996	090/73	213/09	305/14	0.43	8
29	37.231	37.254	029/71	216/19	125/02	0.66	7
30A	38.267	38.278	052/67	236/23	145/02	0.60	10
41	38.097	39.425	127/86	014/02	284/04	0.58	14
45B	38.489	39.283	255/86	045/04	135/02	0.69	6
61	37.458	38.467	182/29	347/60	88/6	0.38	12
67	36.455	38.665	92/66	356/2	265/24	0.94	17
68	36.432	38.585	22/56	190/34	284/6	0.67	13
73D	36.447	37.891	40/63	188/23	284/12	0.76	5
78	34.749	37.287	301/67	80/18	175/14	0.44	12
81B	34.792	37.322	210/65	62/21	328/12	0.31	9
83	34.916	37.497	327/64	190/19	94/16	0.63	21
83C	34.916	37.497	135/80	344/09	253/05	0.33	24
85A	34.995	37.663	340/55	205/27	104/21	0.59	12
85C	34.995	37.663	243/48	34/38	136/15	0.22	5
86B	35.054	37.849	186/47	27/41	288/11	0.41	6
88B	35.235	38.200	200/65	45/23	311/10	0.46	8
93C	36.965	36.846	13/46	268/13	167/41	0.78	6
94B	38.210	38.329	317/17	154/72	49/5	0.98	5
96B	38.702	38.602	124/75	232/4	323/14	0.52	10
100B	38.155	38.317	124/71	226/4	318/18	0.11	9
102B	37.919	38.383	56/70	292/11	199/16	0.31	6
103F	38.628	37.306	086/42	243/36	349/08	0.42	9
105A	38.325	37.474	212/3	104/80	302/10	0.47	25
107A	38.217	37.536	264/56	6/8	101/33	0.35	8
110A	38.005	37.707	359/23	243/46	106/35	0.39	9

*X,Y, coordinates in decimal degrees.
†D/P, direction/plunge.
‡Φ, shape factor.
§N, number of faults.

(Fig. 15). The extension in the region postdates the Campanian to Maastrichtian emplacement of ophiolitic nappes, in the eastern Anatolia, over the Tauride platform (Perinçek & Özkaya 1981; Perinçek & Kozlu 1984; Yiğitbaş & Yılmaz 1996*a*, *b*). Geographically, regional extension during the Paleocene to Eocene reaches as far north as to the Eastern Black Sea Basin. Similarly, Spadini *et al.* (1996) have proposed that Eastern Black Sea Basin was opened as a back-arc basin during the Paleocene to Eocene interval. Therefore, we propose that Paleocene to Eocene extension in the eastern and southeastern Turkey is related to increase in the subduction rates of the southern Branch of the Neotethys (cf. Facenna *et al.* 2001) and decrease in the rate of convergence between Africa and Eurasia *c*. 60 Ma (Dewey *et al.* 1989; Allen *et al.* 2004). This, possibly, gave way to slab roll-back processes and widespread extension, mainly during the Eocene (Robertson *et al.* 2005; Kuscu *et al.* 2010). This extension caused the opening of the Eastern Black Sea Basin and NE–SW stretching of the Tauride Block which gave way to exhumation of metamorphic massifs including Bitlis-Pötürge, Keban and Malatya metamorphics onto which Paleocene to Eocene units are deposited non-conformably (Fig. 20a). On the contrary, Kaymakcı *et al.* (2000, 2003) have reported that during the Late Paleocene to Oligocene interval, western and the north Central Turkey was under compression during which a number of piggy-back basins in the Central Pontides were developed (Gürer & Aldanmaz 2002; Hippolyte *et al.* 2010). This relationship implies

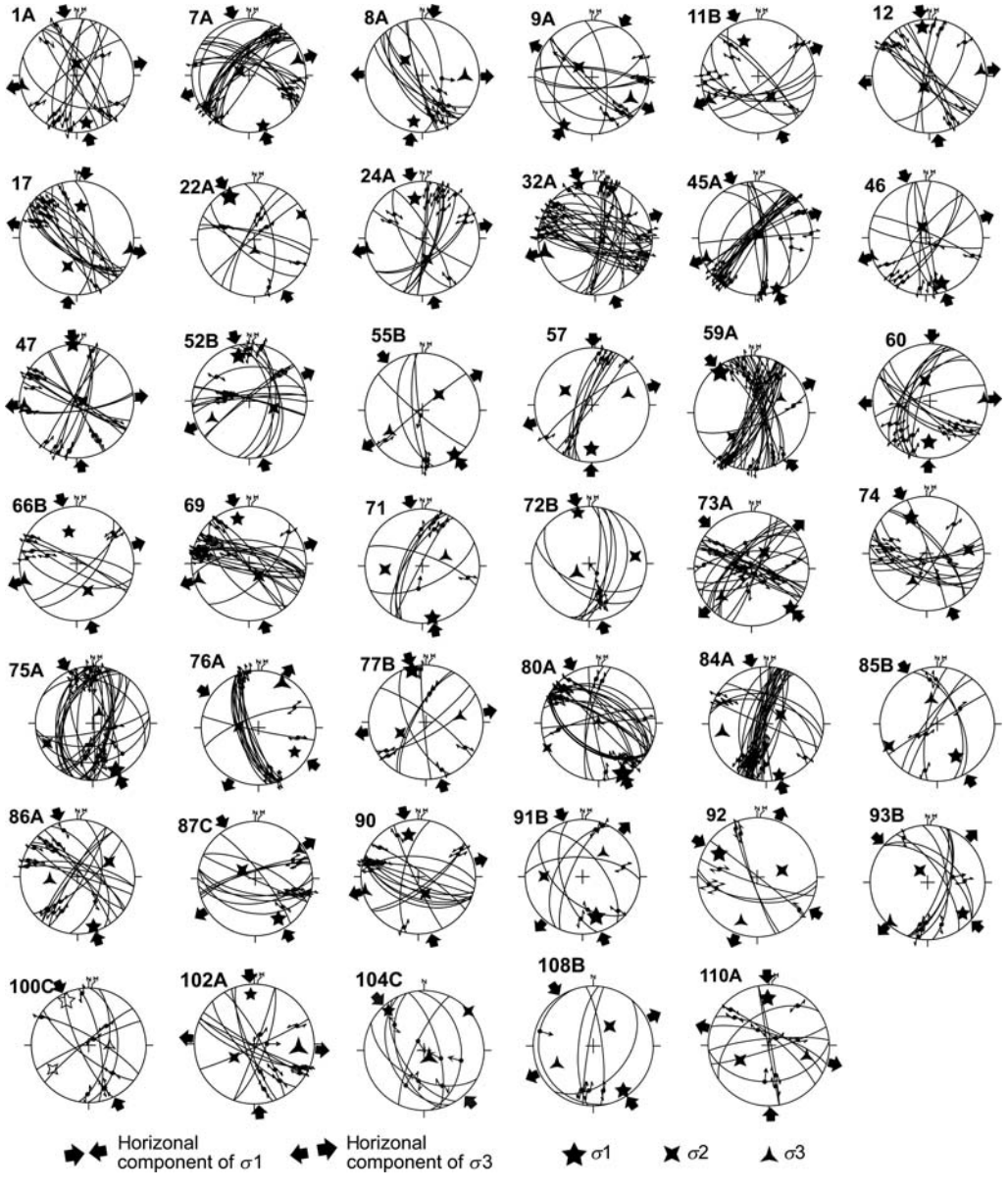

Fig. 11. Palaeostress configurations belonging to the Upper Miocene to Pliocene compression (phase 4). Note that sites 91–108 belong to the Arabian Platform, all others belong to SE Anatolian orogen. Equal area, lower hemisphere projection.

that the tectonic processes in the Eastern Turkey and central north to western Turkey were different during the Paleocene to Eocene interval.

The Paleocene to Eocene extension is replaced by compressional deformation during the Late Eocene to Oligocene (phase 2). During this phase the direction of compression was relatively uniform and orientated NW–SE in the Arabian Platform while it changed from east–west to NNW–SSE north of it (Fig. 16). We believe that the change in the compression directions in the north of the Arabian Plate within the Taurides was possibly due to inversion of some of the Paleocene–Eocene extensional structures and

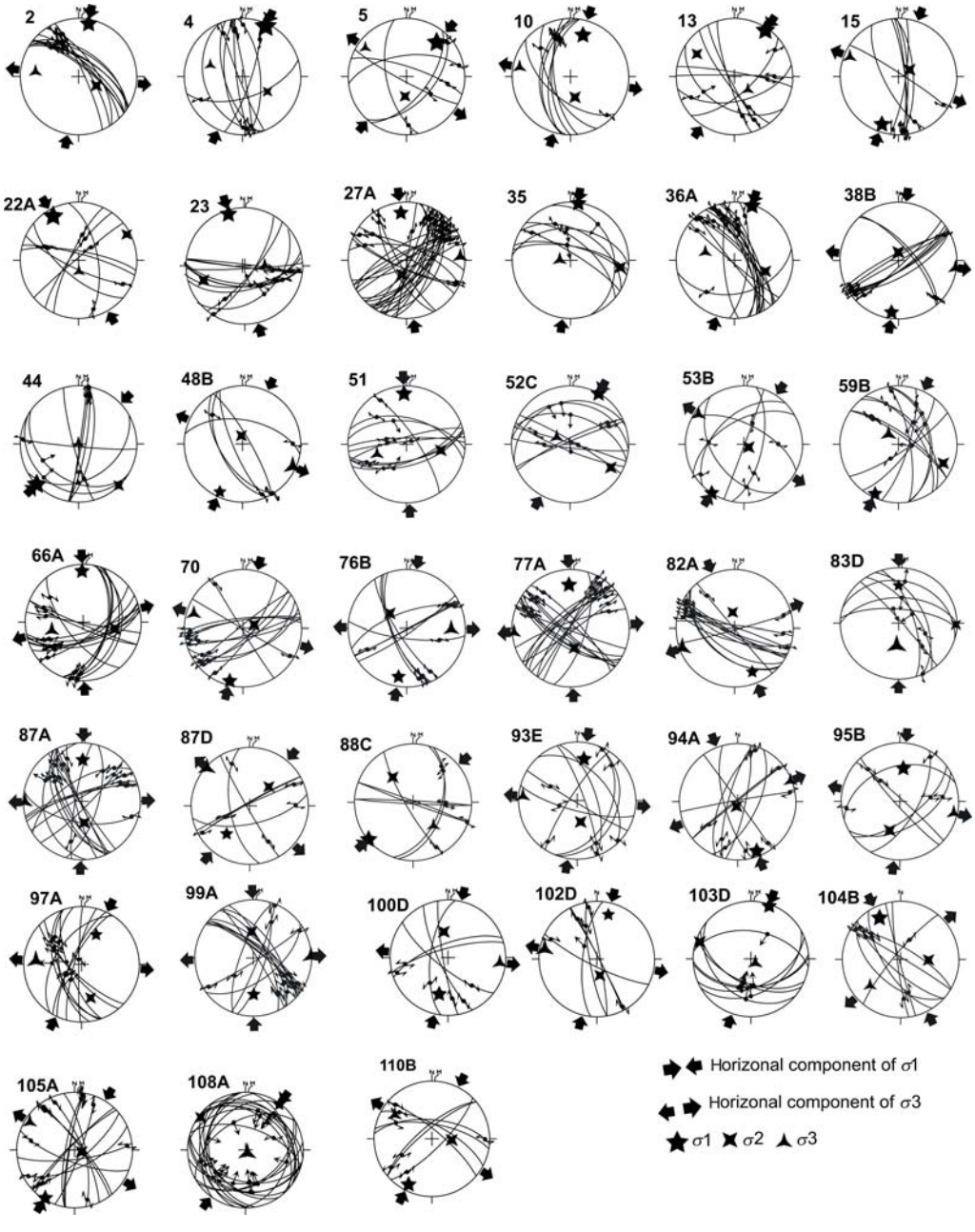

Fig. 12. Palaeostress configurations belonging to late Pliocene to recent compression (phase 5). Note that sites 91–107B belong to the Arabian Platform, all others belong to SE Anatolian orogen. Equal area, lower hemisphere projection.

pervasive internal deformation of the region. Uniform compression directions in the Arabian Plate might indicate lack of major internal deformation which may indicate relative rigidity of the plate.

We speculate that the resumption of compression (Fig. 16) during the Late Eocene–Oligocene interval (Fig. 20b) might be due to subduction of mid-oceanic ridge and/or younger oceanic crust (cf. Hafkenshade *et al.* 2006). It is

Table 4. *Geographical coordinates and palaeostress orientations for the phase 4*

Site code	X*	Y*	σ1 (D/P)†	σ2 (D/P)	σ3 (D/P)	Φ‡	N§
1A	37.321	39.184	169/16	359/74	259/3	0.56	13
7A	37.813	38.991	164/9	294/76	73/11	0.63	25
8A	37.856	38.972	191/19	312/57	91/26	0.64	10
9A	37.981	38.742	210/4	309/66	119/23	0.64	11
11B	39.161	38.674	338/34	147/55	245/05	0.61	10
12	38.959	38.714	352/14	207/73	84/09	0.47	11
17	38.487	39.012	008/43	197/46	102/05	0.62	15
22A	37.849	38.139	330/14	062/07	178/74	0.12	8
23	37.865	38.189	164/13	269/50	064/37	0.32	6
24A	37.957	38.357	349/30	167/60	259/01	0.53	13
32A	38.807	38.427	343/05	102/80	252/09	0.63	32
38	38.097	39.425	188/12	359/78	097/02	0.52	11
45A	38.489	39.283	157/04	038/82	248/07	0.63	23
46	38.100	38.641	161/17	341/73	251/00	0.35	10
47	38.081	38.646	356/01	091/81	266/09	0.40	16
52B	37.373	39.015	347/20	106/53	245/29	0.34	14
55B	37.427	38.688	144/5	46/57	237/33	0.42	5
57	37.413	38.559	181/24	299/46	73/34	0.43	8
59	37.359	38.705	322/12	220/45	63/42	0.09	28
60	37.458	38.467	182/29	347/60	88/6	0.38	16
66	36.450	38.683	359/13	101/43	256/44	0.50	18
66B	36.450	38.683	346/42	157/47	252/4	0.67	7
69	36.503	38.426	346/20	141/68	253/8	0.59	22
71	36.306	38.322	169/9	265/35	67/54	0.38	7
72B	36.465	37.902	347/10	81/20	233/68	0.64	7
73	36.447	37.891	135/4	39/60	227/29	0.39	22
74	36.407	37.822	336/32	85/27	207/45	0.41	13
75	35.835	37.539	154/10	246/14	31/73	0.21	27
75B	35.835	37.539	139/37	329/52	233/5	0.02	7
76	35.903	37.823	124/25	273/62	28/13	0.81	14
77B	35.873	37.856	345/7	247/50	80/39	0.26	8
80	34.813	37.209	154/3	244/1	353/87	0.01	24
84	34.990	37.649	166/8	57/65	259/23	0.61	33
85B	34.995	37.663	150/35	246/8	346/53	0.45	6
86	35.054	37.849	162/10	65/39	264/50	0.45	16
87C	35.141	38.172	150/20	304/68	57/9	0.43	12
90	35.354	38.152	347/26	157/64	255/4	0.52	14
91B	37.282	37.022	156/5	254/58	63/32	0.19	5
93B	36.965	36.846	131/19	327/70	223/5	0.57	8
94A	38.451	38.770	159/10	322/79	68/3	0.41	9
99A	38.266	38.271	179/38	357/52	88/1	0.70	16
100C	37.666	36.991	333/14	237/26	90/60	0.29	8
102A	37.919	38.383	82/72	214/12	307/13	0.59	7
103A	38.628	37.306	72/19	335/18	204/63	0.58	7
103D	38.628	37.306	151/32	247/ 9	350/57	0.72	17
104A	38.497	37.368	262/12	358/26	149/61	0.56	15
104B	38.497	37.368	333/21	91/50	229/32	0.35	8
104C	38.497	37.368	318/12	48/1	145/78	0.77	7
108A	38.160	37.720	36/2	306/4	148/85	0.78	22
108B	38.160	37.720	146/11	40/55	243/33	0.44	8

*X,Y, coordinates in decimal degrees.
†D/P, direction/plunge.
‡Φ, shape factor.
§N, number of faults.

Table 5. *Geographical coordinates and palaeostress orientations for the phase 5*

Site code	X*	Y*	σ1 (D/P)†	σ2 (D/P)	σ3 (D/P)	Φ‡	N§
2	37.473	39.166	11/8	117/62	277/27	0.31	11
4	37.668	39.082	25/6	121/49	290/41	0.04	10
5	37.703	39.057	41/25	184/62	305/15	0.16	6
10	38.047	38.722	17/26	168/60	280/12	0.34	7
13	38.817	38.736	34/5	301/26	134/64	0.16	8
15	38.692	38.827	199/14	58/72	292/11	0.38	7
22A	37.849	38.139	330/14	062/07	178/74	0.12	8
23	37.865	38.189	164/13	269/50	064/37	0.32	6
27A	37.512	37.059	004/59	178/31	269/03	0.50	30
35	37.151	37.303	008/02	098/15	272/75	0.40	7
36A	38.328	38.644	018/02	110/43	286/47	0.30	18
38	38.097	39.425	188/12	359/78	097/02	0.52	11
44	38.489	39.283	226/00	136/01	338/89	0.16	9
48B	37.976	38.745	205/10	352/781	114/06	0.80	5
51	37.356	39.028	357/14	100/40	252/46	0.37	13
52C	37.373	39.015	29/0	119/21	298/69	0.42	9
53B	37.442	38.968	213/0	121/82	303/8	0.51	6
59B	37.359	38.705	271/25	97/65	2/3	0.44	10
70	36.406	38.281	194/8	73/74	286/14	0.50	13
76B	35.903	37.823	190/18	311/59	91/25	0.60	9
77	35.873	37.856	358/27	169/63	266/4	0.42	22
82A	34.877	37.470	149/43	358/43	254/15	0.86	12
83D	34.916	37.497	13/80	103/0	193/10	0.83	7
87	35.141	38.172	1/30	174/60	269/3	0.59	16
87D	35.141	38.172	220/38	45/52	312/3	0.77	6
88C	35.235	38.200	230/1	321/44	139/46	0.32	24
88D	35.235	38.200	5/46	106/10	205/42	0.80	7
91B	37.282	37.022	156/5	254/58	63/32	0.20	5
93B	36.965	36.846	131/19	327/70	223/5	0.57	8
93E	36.970	36.807	10/17	171/60	275/8	0.49	8
94A	38.451	38.770	159/10	322/79	68/3	0.41	9
94B	38.210	38.329	317/17	154/72	49/5	0.98	5
95B	38.618	38.839	158/58	199/46	102/7	0.46	7
99A	38.266	38.271	179/38	357/52	88/1	0.70	16
102A	37.919	38.383	82/72	214/12	307/13	0.58	7
104B	38.497	37.368	333/21	91/50	229/32	0.35	8
108C	38.160	37.720	146/11	40/55	243/33	0.44	8

*X,Y, coordinates in decimal degrees.
†D/P, direction/plunge.
‡Φ, shape factor.
§N, number of faults.

important to note that the Late Eocene–Oligocene compression is very widespread and extends from eastern Turkey to Aegean region (Şengör & Yılmaz 1981; Okay *et al.* 2001) and further west into Greece (Van Hinsbergen *et al.* 2005). As an indirect evidence for the Late Eocene–Oligocene compression, during this time interval, most areas in Turkey is characterized generally by erosion and period of local continental deposition (Kaymakcı 2000; Gürer & Aldanmaz 2002) which might be coupled with aridification and sea level drop (cf. Dupont-Nivet *et al.* 2007).

Starting from the latest Oligocene, the Early Miocene is characterized by widespread shallow marine deposition in eastern and south-eastern Turkey which was previously covered by Upper Eocene to Oligocene continental deposits. During this time interval, most of the north–NE- to south–SW-trending normal faults were developed under east–west to NW–SE orientated extension (phase 3, Figs 17 & 20c). The tectonic cause of Lower Miocene extension is thought to relate with the westwards migration of detached slab which started in Iran during the Oligocene and reached to south-eastern Turkey during the Middle Miocene. This gave way to a short period of localized extension that the topography of eastern Turkey was about sea level. Topographical lowering is followed by uplift

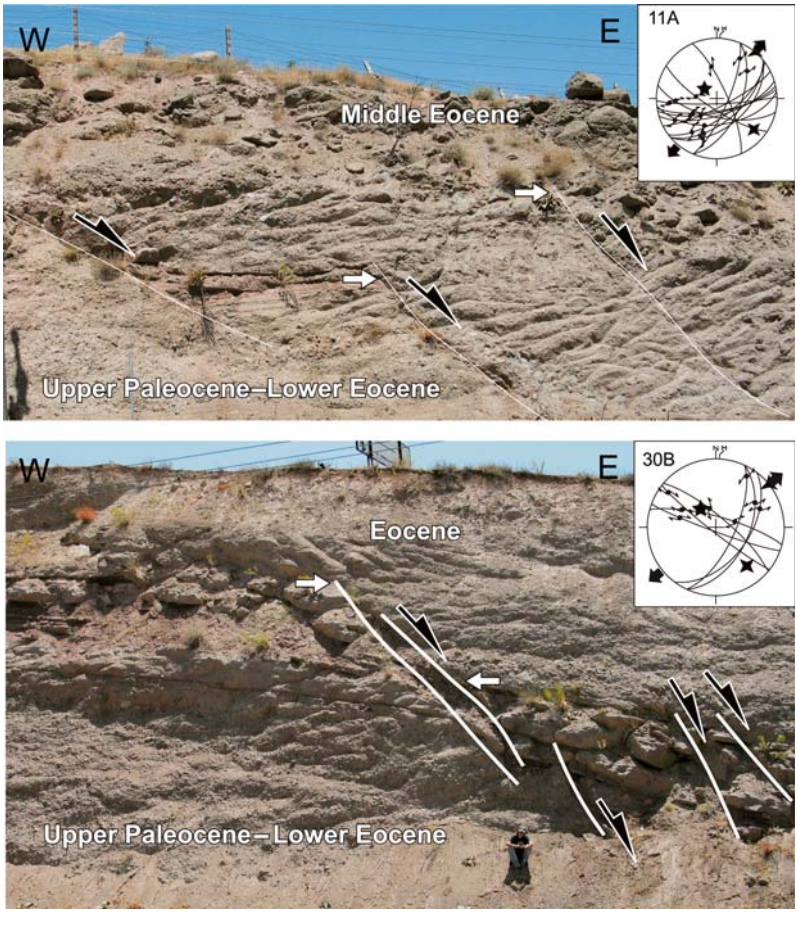

Fig. 13. Growth faults developed within the Lower Eocene units and resultant stress configuration (sites 11A and 30B in Fig. 6, view to north).

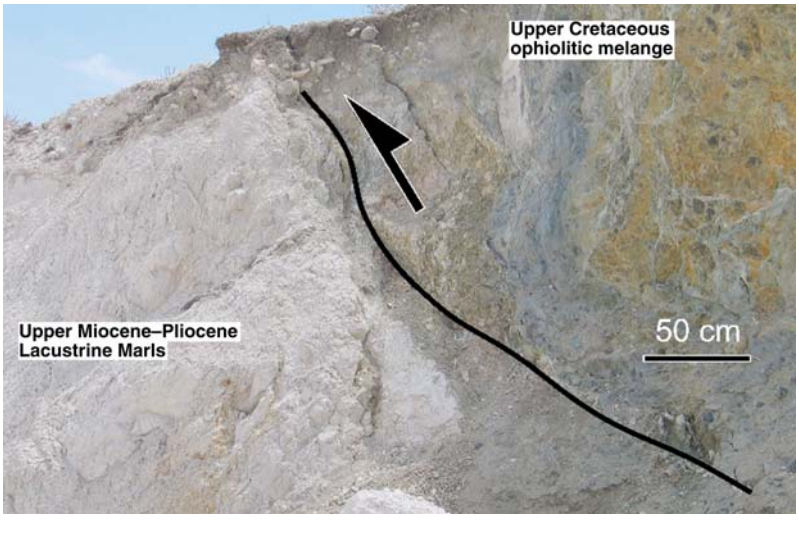

Fig. 14. Close-up view of the southern boundary thrust fault of the Kangal Basin (location 51 in Fig. 6).

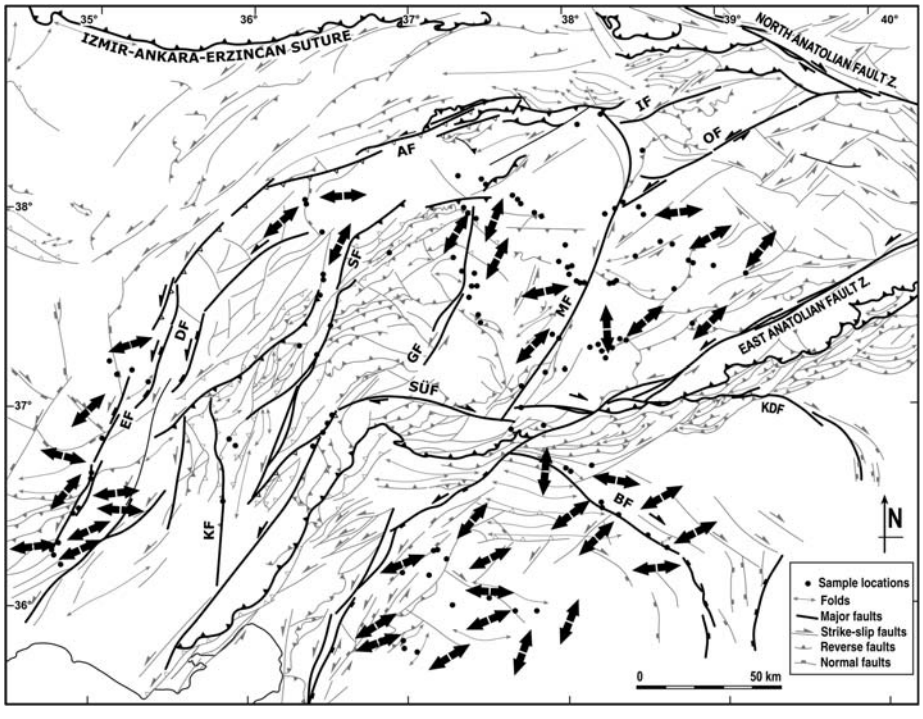

Fig. 15. Major structures and extension directions (i.e. horizontal component of σ_3) in south-eastern Turkey for the Late Paleocene to Middle Eocene period which corresponds to deformation phase 1. Deviations from NE–SW extension are possibly due to block rotations in the successive deformation phases.

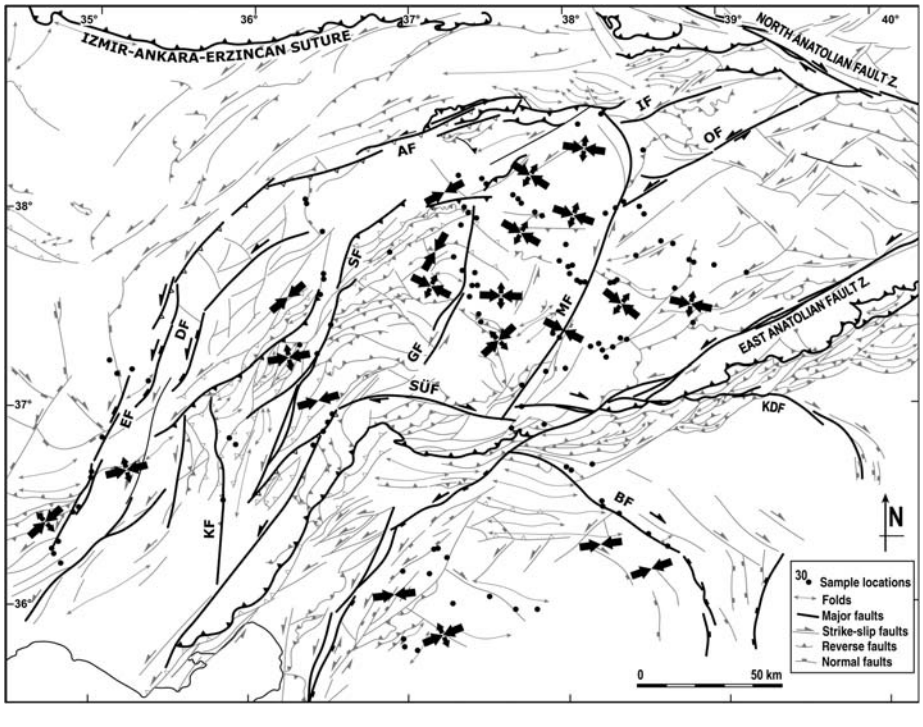

Fig. 16. Late Eocene to Oligocene compression (large arrows) and extension (small arrows) directions (i.e. horizontal components of σ_1 and σ_3) in southeastern Turkey.

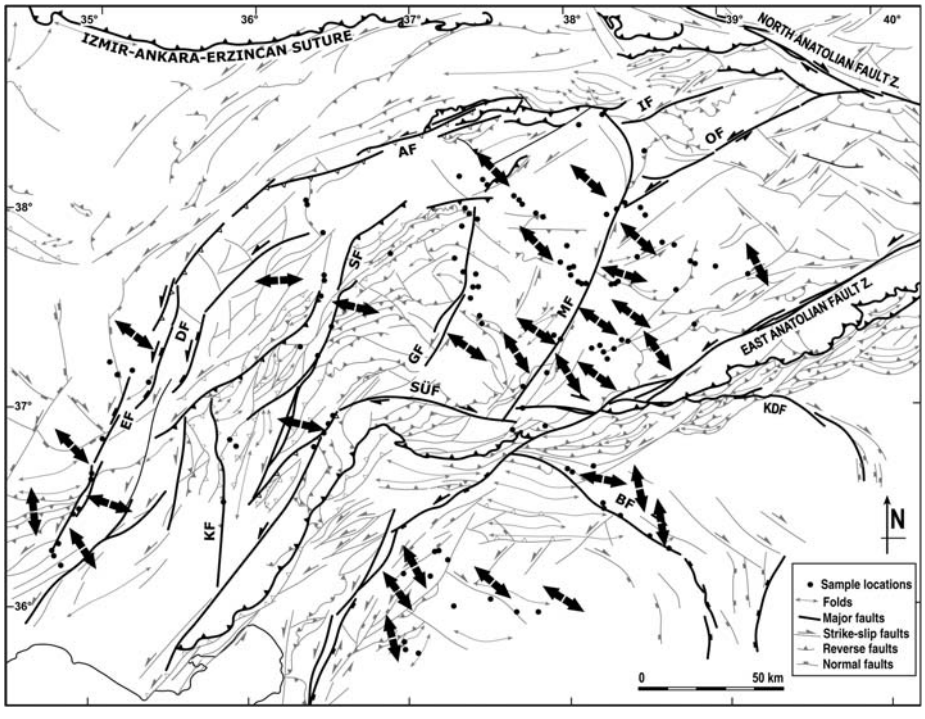

Fig. 17. Latest Oligocene–Middle Miocene extension directions (i.e. horizontal component of σ_3) in southeastern Turkey.

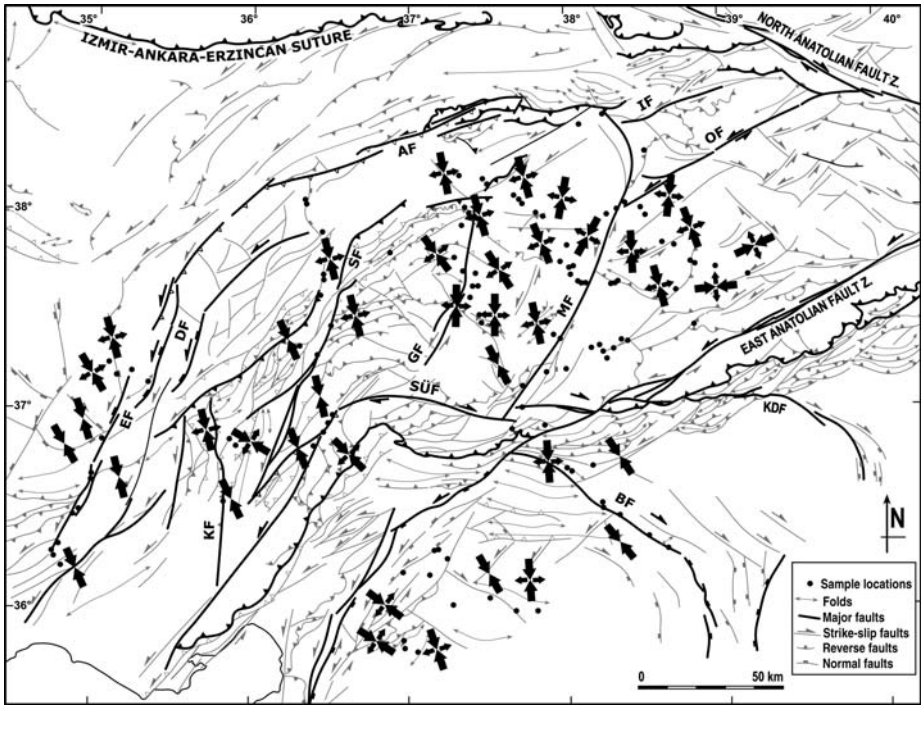

Fig. 18. Upper Miocene to Pliocene (phase 4) compression (large arrows) and extension (small arrows) directions (i.e. horizontal components of σ_1 and σ_3) in southeastern Turkey.

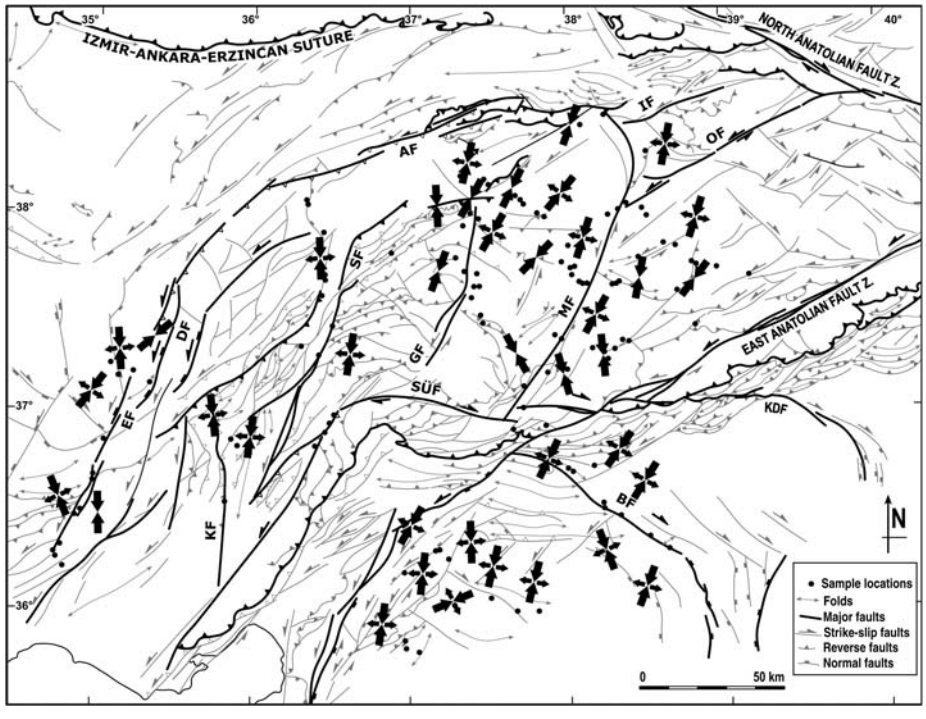

Fig. 19. Upper Pliocene to Recent (phase 5) compression (large arrows) and extension (small arrows) directions (i.e. horizontal components of σ_1 and σ_3) in southeastern Turkey. As compared to Figure 18 there is slight but significant variation in the σ_3 directions. This variation is possibly due to tectonic reorganization in eastern Turkey related to eastwards jump of the junction between the north and east Anatolian fault Zones as proposed by Westaway & Arger (2001).

as the detachment migrated westwards (cf. Buiter *et al.* 2002). This gave way to continental deposition in Malatya (Kaymakcı *et al.* 2006; Türkmen *et al.* 2007), and adjacent basins in the north of the Bitlis Suture while foreland flysch deposition continued south of it (Perinçek & Özkaya 1981; Karig & Kozlu 1990; Huesing *et al.* 2009).

The deformation phase 4 (Fig. 18) is related to the collision and further northwards convergence of the Arabian Plate into the Eurasian Plate. The beginning of the collision is generally accepted as the end of Serravalian (11 Ma) based on the youngest marine deposition in south–east Anatolia (Şengör & Yılmaz 1981) which coincides with Middle Miocene climate transition (Huesing *et al.* 2009). The collision gave way to approximately north–south compression; crustal thickening (Dewey *et al.* 1986) and westwards escape of Anatolian Block (Şengör *et al.* 1985). During the Middle Pliocene (*c*. 3.5 Ma) a tectonic reorganization occurred in the region which might be related to the complete emergence of the North and the East Anatolian fault zones as independent lithospheric structures. This resulted in slight but relatively significant change in the stress configurations (phase 5, Fig. 19) coupled with the westwards escape of the Anatolia and eastwards jump of the junction between the north and east Anatolian fault Zones as proposed by Westaway & Arger (2001).

Conclusions

This study has reached following conclusions.

- The Arabian Platform and the SE Anatolian orogen have evolved into five different deformation phases.
- The oldest deformation phase took place during the Paleocene to Middle Eocene interval and is characterized by NE–SW extensional deformation resulted from roll-back of northwards subducting southern branch of the Neotethys lithosphere.
- The second deformation phase took place during the Late Eocene to Oligocene interval and is characterized by east–west to NW–SE compression resulted from termination of roll-back

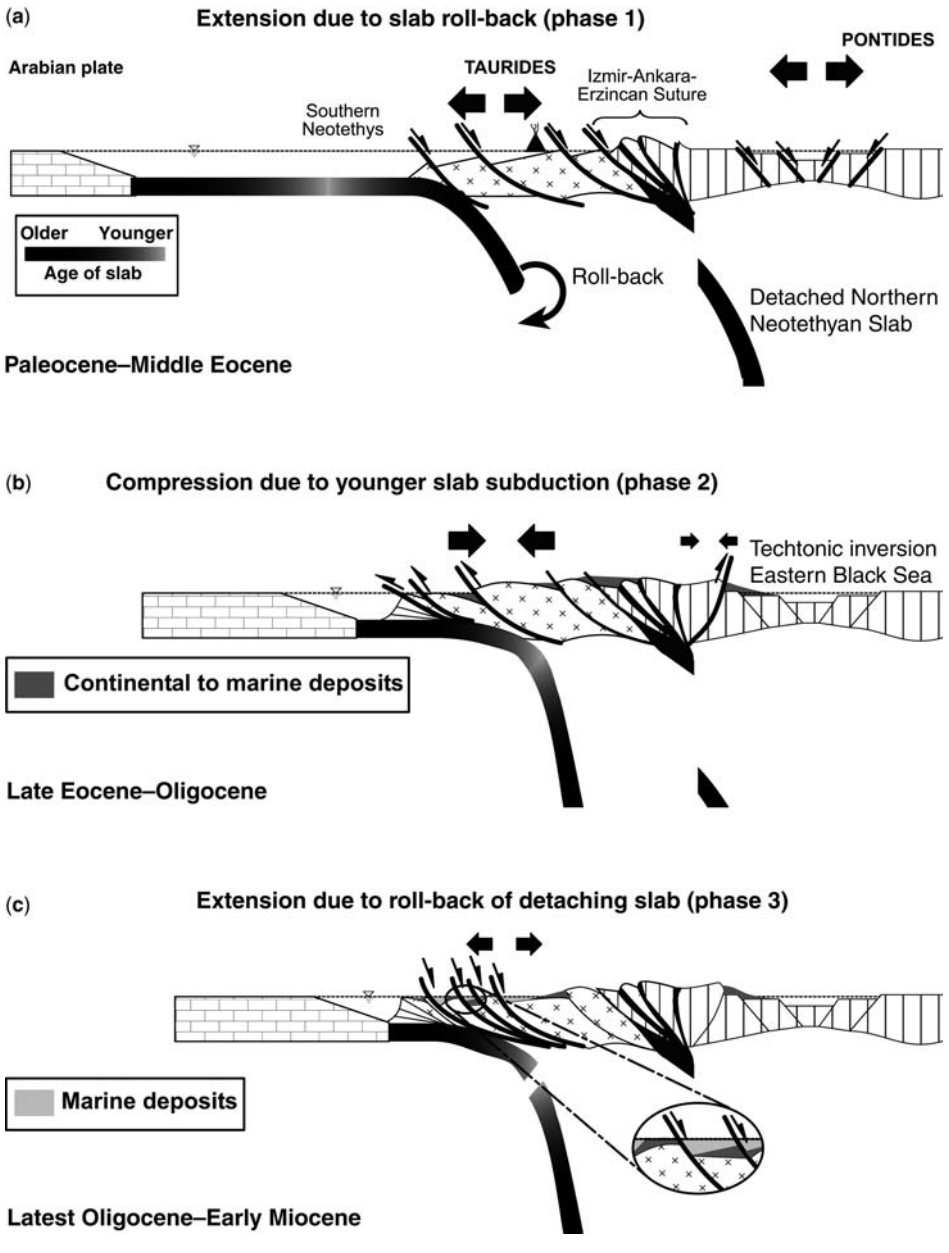

Fig. 20. Two dimensional approximately north–south orientated conceptual cross-sections from Eastern Black Sea to Arabian Platform explaining the Paleocene to Early Miocene evolution of the region. (**a**) Slab roll-back process during the Paleocene to Middle Eocene in eastern Turkey resulted in far reaching extensional deformation in eastern Turkey which also resulted in the opening of the Eastern Black Sea Basin. During this time interval extension on the Arabian Platform was due to slab-pull forces of the down-going slab. (**b**) During the Late Eocene to Oligocene convergence between Pontides and Arabian Plate resumed and due to subduction of relatively younger and lighter oceanic crust gave rise to compressional deformation in the region (both on the Arabian and over-riding plates). (**c**) Towards end of Oligocene slab started to detach, this gave way to short time subsidence (as evidenced by Early Miocene marine deposits i.e. Adilcevaz Fm.) followed by uplift of the over-riding plate that resulted in uplift of the basins while extensional deformation was prevailed. This gave rise to continental deposition characterized mainly by fluvio-lacustrine environments (e.g. Gürün, Malatya, Kangal and Sivas basins). In the south, marine deposition along the trench continued until the end of Middle Miocene (Kaymakcı *et al.* 2006; Huesing *et al.* 2009).

possibly due to subduction of younger oceanic lithosphere.

- The third deformation phase took place during the Latest Oligocene to Middle Miocene interval and characterized by NW–SE directed extension resulted from west wards migrating detachment of the Neotethyan lithosphere.
- The fourth and fifth deformation phases are relate to terminal subduction that gave way to collision and indentation of Arabian Plate into the Eurasian Plate and complete emergence of north and east Anatolian faults zones as independent lithospheric structures.

This study is supported by Middle East Basins Evolution (MEBE) project between 2003–2005. We would like to thank Ilkay Kuşcu for fruitful discussions about the evolution of Tethys system.

References

Allen, M., Jackson, J. & Walker, R. 2004. Late Cenozoic reorganization of the Arabia-Eurasia collision and the comparison of short-term and long-term deformation rates. *Tectonics*, **23**, 1–16.

Anderson, E. M. 1951. *The Dynamics of Faulting*. Oliver and Boyd, Edinburgh.

Angelier, J. 1988. Tector: Determination of stress tensor using fault slip data set. *Quantitative Tectonics*, University Pierre and Marie Curie, Paris.

Angelier, J. 1994. Fault slip analysis and palaeostress reconstruction. *In*: Hancock, P. L. (ed.) *Continental Deformation*. Pergamon Press, Oxford, 53–100.

Arger, J., Mitchell, J. & Westaway, R. 2000. Neogene and Quaternary volcanism of south-eastern Turkey. *In*: Bozkurt, E., Winchester, J. A. & Piper, J. D. A. (eds) *Tectonics and Magmatism, in Turkey and the Surrounding Area*. Geological Society, London, Special Publications, **173**, 459–487.

Aziz, A., Erakman, B., Kurt, G. & Meşhur, M. 1982. *Pınarbaşı-Sarız-Gürün ilçeleri arasında kalan alanın jeoloji raporu*. TPAO Rapor No. **1601** (unpublished).

Bayarslan, M. & Bingöl, A. F. 2000. Petrology of a supra-subduction zone ophiolite (Elazığ-Turkey). *Canadian Journal of Earth Sciences*, **37**, 1411–1424.

Bott, M. P. H. 1959. The mechanics of oblique-slip faulting. *Geological Magazine*, **96**, 109–117.

Buiter, S. J. H., Govers, R. & Wortel, M. J. R. 2002. Two-dimensional simulations of surface deformation caused by slab detachment. *Tectonophysics*, **354**, 195–210.

Dewey, J. F., Helman, M. L., Turco, E., Hutton, D. H. W. & Knott, S. D. 1989. Kinematics of the western Mediterranean. *In*: Coward, M. P., Dietrich, D. & Park, R. G. (eds) *Alpine Tectonics*. Geological Society, London, Special Publications, **45**, 265–283.

Dewey, J. F., Hempton, M. R., Kidd, W. S. F., Şaroglu, F. & Şengor, A. M. C. 1986. Shortening of continental lithosphere: the neotectonics of Eastern Anatolia – a young collision zone. *In*: Coward, A. C. & Ries, M. P. (eds) *Collision Tectonics*. Geological Society, London, Special Publications, **19**, 3–36.

Dupont-Nivet, G., Krijgsman, W., Langereis, C. G., Abels, H. A., Dai, S. & Fang, X. 2007. Tibetan Plateau Aridification linked to global cooling at the Eocene-Oligocene transition. *Nature*, **445**, 635–638.

Faccenna, C., Becker, T. W., Lucente, F. P., Jolivet, L. & Rossetti, F. 2001. History of subduction and back-arc extension in the Central Mediterranean. *Geophysical Journal International*, **145**, 809–820.

Faccenna, G., Bellier, O., Martinod, J., Piromallo, C. & Regard, V. 2005. Slab detachment beneath eastern Anatolia: a possible cause for the formation of the North Anatolian fault. *Earth and Planetary Science Letters*, **242**, 85–97.

Görür, N., Oktay, F. Y., Seymen, I. & Şengör, A. M. C. 1984. Palaeotectonic evolution of the Tuzgölü basin complex, Central Turkey: sedimentary record of a neotethyan closure. *In*: Dixon, J. E. & Robertson, A. H. F. (eds) *The Geological Evolution of the Eastern Mediterranean*. Geological Society, London, Special Publications, **17**, 455–466.

Govers, R. & Wortel, M. J. R. 2005. Lithosphere tearing at STEP faults: response to edges of subduction zones. *Earth and Planetary Science Letters*, **236**, 505–523.

Gürer, O. F. & Aldanmaz, E. 2002. Origin of the Upper Cretaceous – Tertiary sedimentary basins within the Tauride – Anatolide platform in Turkey. *Geological Magazine*, **139**, 191–197.

Hafkenscheid, E., Wortel, M. J. R. & Spakman, W. 2006. Subduction history of the Tethyan region derived from seismic tomography and tectonic reconstructions. *Journal of Geophysical Research*, **111**, B08401, doi: 10.1029/2005JB003791.

Hippolyte, J.-C., Müller, C., Kaymakci, N. & Sangu, E. 2010. Dating of the Black Sea Basin: new nannoplankton ages from its inverted margin in the Central Pontides (Turkey). *In*: Sosson, M., Kaymakci, N., Stephenson, R. A., Bergerat, F. & Starostenko, V. (eds) *Sedimentary Basin Tectonics from the Black Sea and Caucasus to the Arabian Platform*. Geological Society, London, Special Publications, **340**, 113–136.

Huesing, S. K., Zachariasse, W. J. *et al.* 2009. Oligo-Miocene foreland basin evolution in SE Anatolia: implications for the closure of the eastern Tethys gateway. *In*: Van Hinsbergen, D. J. J., Edwards, M. A. & Govers, R. (eds) *Geodynamics of Collision and Collapse at the Africa–Arabia–Eurasia Subduction Zone*. Geological Society, London, Special Publications, **311**, 107–132.

Karig, D. E. & Kozlu, H. 1990. Late Palaeogene evolution of the triple junction region near Maraş, south-central Turkey. *Journal of the Geological Society, London*, **147**, 1023–1034.

Kaymakci, N., White, S. H. & van Dijk, P. M. 2000. Paleostress inversion in a multiphase deformed area: kinematic and structural evolution of the Çankiri Basin (central Turkey), Part 1. *In*: Bozkurt, E., Winchester, J. A. & Piper, J. A. D. (eds) *Tectonics and Magmatism in Turkey and the Surrounding Area*. Geological Society, London, Special Publications, **173**, 445–473.

Kaymakci, N., White, S. H. & van Dijk, P. M. 2003. Kinematic and structural development of the Çankiri

Basin (Central Anatolia, Turkey): a paleostress inversion study. *Tectonophysics*, **364**, 85–113.

KAYMAKCI, N., İNCEÖZ, M. & ERTEPINAR, P. 2006. 3D-architecture and Neogene evolution of the Malatya Basin: inferences for the kinematics of the Malatya and Ovacık fault zones. *Turkish Journal of Earth Sciences*, **15**, 123–154.

KAYMAKCI, N., ÖZÇELIK, Y., WHITE, S. H. & VAN DIJK, P. M. 2009. Tectono-stratigraphy of the Çankırı Basin: Late Cretaceous to Early Miocene evolution of the Neotethyan Suture Zone in Turkey. *In*: VAN HINSBERGEN, D. J. J., EDWARDS, M. A. & GOVERS, R. (eds) *Geodynamics of Collision and Collapse at the Africa–Arabia–Eurasia Subduction Zone*. Geological Society, London, Special Publications, **311**, 67–106.

KETIN, İ. 1966. Anadolu'nun tektonik birlikleri. *Maden Tetkik ve Arama Enstitüsü Dergisi*, **66**, 20–34.

KUSÇU, İ., GENÇALIOĞLU-KUŞCU, G., TOSDAL, R. M., ULRICH, T. D. & FRIEDMAN, R. 2010. Magmatism in the southeastern Anatolian orogenic belt: transition from arc to post-collisional setting in an evolving orogen. *In*: SOSSON, M., KAYMAKCI, N., STEPHENSON, R. A., BERGERAT, F. & STAROSTENKO, V. (eds) *Sedimentary Basin Tectonics from the Black Sea and Caucasus to the Arabian Platform*. Geological Society, London, Special Publications, **340**, 437–460.

OKAY, A. İ., ŞENGÖR, A. M. C. & GÖRÜR, N. 1994. Kinematic history of the opening of the Black Sea and its effect on the surrounding regions. *Geology*, **22**, 267–270.

OKAY, A. I., TANSEL, İ. & TÜYÜSZ, O. 2001. Obduction, subduction and collision as reflected in the Upper Cretaceous–Lower Eocene sedimentary record of western Turkey. *Geological Magazine*, **138**, 117–142.

PARLAK, O. 2005. Geodynamic significance of granitoid magmatism in the southeast Anatolian orogen: geochemical and geochronogical evidence from Goksun–Afsin (Kahramanmaras, Turkey) region. *International Journal of Earth*, **95**, 609–627.

PARLAK, O., HOCK, V., KOZLU, H. & DELALOYE, M. 2004. Oceanic crust generation in an island arc tectonic setting, SE Anatolian orogenic belt (Turkey). *Geological Magazine*, **141**, 583–603.

PARLAK, O., YILMAZ, H. & BOZTUG, D. 2006. Origin and tectonic significance of the metamorphic sole and isolated dykes of the Divrigi ophiolite (Sivas, Turkey): evidence for slab break-off prior to ophiolite emplacement. *Turkish Journal of Earth Sciences*, **15**, 25–45.

PEARCE, J. A., BENDER, J. F. *ET AL.* 1990. Genesis of collision volcanism in Eastern Anatolia, Turkey. *Journal of Volcanology and Geothermal Research*, **44**, 189–229.

PERINÇEK, D. 1979. Geological investigation of the Çelikhan-Sincik-Koçali area (Adıyaman province). *İstanbul Universitesi Fen Fakültesi Mecmuası, Seri B*, **44**, 127–147.

PERINÇEK, D. & KOZLU, H. 1984. Stratigraphical and structural relations of the units in the Afşin-Elbistan-Doğanşehir region (Eastern Taurus). *In*: TEKELI, O. & GONCUOGLU, M. C. (eds) *Geology of the Taurus Belt*. Proceedings of International Symposium. MTA, Ankara, 181–198.

PERINÇEK, D. & ÖZKAYA, I. 1981. Tectonic evolution of the northern margin of the Arabian plate. *Hacettepe University Bulletin of Earth Sciences*, **8**, 91–101.

PERINÇEK, D., GÜNAY, Y. & KOZLU, H. 1987. New observations about the strike-slip faults in east and southeast Anatolia. *In*: Organizing Committee of Turkish Association of Petroleum Geologists (eds) *Proceedings of the 7th Turkish Petroleum Congress*, 89–103.

ROBERTSON, A. H. F. 2002. Overview of the genesis and emplacement of Mesozoic ophiolites in the Eastern Mediterranean Tethyan region. *Lithos*, **65**, 1–67.

ROBERTSON, A. H. F., USTAÖMER, T., PARLAK, O., ÜNLÜGENÇ, U. C., TAŞLI, K. & İNAN, N. 2005. Late Cretaceous–Early Tertiary tectonic evolution of south-Neotethys in SE Turkey: evidence from the Tauride thrust belt in SE Turkey (Binboga-Engizek segment). *Journal of Asian Earth Sciences*, **27**, 108–145.

ŞENGÖR, A. M. C. & YILMAZ, Y. 1981. Tethyan evolution of Turkey. A plate tectonic approach. *Tectonophysics*, **75**, 181–241.

ŞENGÖR, A. M. C., GORUR, N. & ŞAROĞLU, F. 1985. Strike-slip faulting and related basin formation in zones of tectonic escape: Turkey as a case study. *In*: BIDDLE, K. T. & CHRISTIE-BLICK, N. (eds) *Strike-Slip Deformation, Basin Formation and Sedimentation*. Society of Economic Paleontology and Mineralogy, Special Publications, **37**, 227–264.

SPADINI, G., ROBINSON, A. & CLOETINGH, S. 1996. Western versus Eastern Black Sea tectonic evolution: pre-rift lithospheric controls on basin formation. *Tectonophysics*, **266**, 139–154.

STAMPFLI, G. M. & BOREL, G. D. 2002. A plate tectonic model for the Paleozoic and Mesozoic constrained by dynamic plate boundaries and restored synthetic oceanic isochrons. *Earth and Planetary Science Letters*, **196**, 17–33.

SUNGURLU, O. 1974. Geology of the northern part of petroleum district – VI. *2nd Petroleum Congress of Turkey*. Turkish Association of Petroleum Geologists, 85–107.

TATAR, O., PIPER, J. D. A., GÜRSOY, H., HEIMANN, A. & KOÇBULUT, F. 2004. Neotectonic deformation in the transition zone between the Dead Sea Transform and the east Anatolian fault Zone, Southern Turkey: a palaeomagnetic study of the Karasu Rift Volcanism. *Tectonophysics*, **385**, 17–43.

TUNA, D. 1973. VI. Bolge litostratigrafi adlamasının açıklayıcı raporu. TPAO Rapor No. **813**, 131 (unpublished).

TÜRKMEN, İ., AKSOY, E., KOÇ, C. & TAŞGIN, C. 2007. Alluvial and lacustrine facies in an extensional basin: the Miocene of Malatya basin, eastern Turkey. *Journal of Asian Earth Sciences*, **30**, 181–198.

TÜYSÜZ, O. 1999. Geology of the Cretaceous sedimentary basins of the Western Pontides. *Geological Journal*, **34**, 75–93.

ULU, Ü, GENÇ, Ş. *ET AL.* 1991. *Belveren-Araban-Yavuzeli-Nizip-Birecik dolayının jeolojisi ve Senozoyik yaşlı volkanik kayaçların petrolojisi ve bölgesel yayılımı.* Maden Tetkik ve Arama Raporu No: **9226** (unpublished).

VAN HINSBERGEN, D. J. J., HAFKENSCHEID, E., SPAKMAN, W., MEULENKAMP, J. E. & WORTEL, M. J. R. 2005. Nappe stacking resulting from subduction of oceanic and continental lithosphere below Greece. *Geology*, **33**, 325–328.

WALLACE, R. E. 1951. Geometry of shearing stress and relation to faulting. *Journal of Geology*, **69**, 118–130.

WESTAWAY, R. & ARGER, J. 2001. Kinematics of the Malatya-Ovacık fault zone. *Geodynamica Acta*, **14**, 103–131.

WILSON, H. H. & KRUMMENACHER, R. 1957. *Geology and Oil Prospects of the Gaziantep Region, Southeast Turkey*. TPAO Report No. **839** (unpublished).

YAZGAN, E. & CHESSEX, R. 1991. Geology and tectonic evolution of the Southeastern Taurus in the region of Malatya. *Turkish Association of Petroleum Geologists Bulletin*, **3**, 1–42.

YIĞITBAŞ, E. & YILMAZ, Y. 1996*a*. New evidence and solution to the Maden complex controversy of the southeast Anatolian orogenic belt (Turkey). *Geologisches Rundschau*, **85**, 250–263.

YIĞITBAŞ, E. & YILMAZ, Y. 1996*b*. Post-late Cretaceous strike-slip tectonics and its implications for the Southeast Anatolian orogen, Turkey. *International Geology Review*, **38**, 818–831.

YILMAZ, Y. 1993. New evidence and model on the evolution of the Southeast Anatolian orogen. *Geological Society of America Bulletin*, **105**, 251–271.

YOLDEMIR, O. 1987. *Suvarlı-Haydarlı-Narlı-Gaziantep arasında kalan alanın jeolojisi yapısal durumu ve Petrol olanakları.* TPAO Rapor No: **2257**.